Research Paper

Climate, paleohydrology and land use change in the Central Iberian Range over the last 1.6 ka: The La Parra Lake record

Fernando Barreiro-Lostres[1], Ana Moreno[1], Santiago Giralt[2], Margarita Caballero[3] and Blas Valero-Garcés[1]

Abstract

A multiproxy study of a 7 m long sedimentary sequence from Lake La Parra (39º 50.948', 1º 52', 1014 m a.s.l) supported by 11 ^{14}C AMS and $^{210}Pb/^{137}Cs$ dates provides a robust, high-resolution hydrological and environmental variability record for the last 1600 years of the Las Torcas sinkhole Complex in the Central Iberian Range. The succession of depositional environments in Lake La Parra sinkhole is controlled by both changes in the regional water table and by the balance between sedimentary input through ephemeral creeks and in-lake production of carbonates and organic matter. Although synergetic links with climate are likely, phases of increased sediment delivery to the lake at ca 500–700 AD, ca 1000 AD, 1450-1500 AD, 1550-650 AD and since 1700 till recent times are driven primarily by human impact in the watershed. Prior to ca 300 AD the sinkhole was dry, then became a lake at the end of the Roman Period (350 AD) when the doline was flooded, and it has not dried out during the last 1600 years. Moderate lake levels with deposition of coarser clastic facies dominated up to the 12th century (400-1200 AD), and relatively higher levels with deposition of laminated facies during the 13th-15th centuries (1200-1600 AD). The pattern of paleohydrological evolution at a centennial scale is roughly coherent with most Iberian lacustrine records, however, the 'La Parra' sequence indicates that increased humidity during Iberian-Roman times was restricted to southern Spain, and the humid phases of the LIA starting and ending earlier in the central Iberian Range compared to the Pyrenean Domain and southern Spain. This new sequence highlights the heterogeneity through space and time of the main dry and wet climatic periods at shorter scales, emphasizing the impact of latitudinal climate gradients on the Iberian Peninsula climate variability.

Keywords

Late Holocene, sedimentary facies geochemistry, diatoms, Iberian Peninsula, karstic lake, palaeohydrology, human impact.

Revised manuscript accepted 21 April 2014

Introduction

Late Holocene palaeoclimate reconstructions are critical improving our understanding of current climate variability and predictions of environmental responses to future climate changes (Bradley et al., 2003; Mayewski et al., 2004; Mann et al., 2009; Jones et al., 2009). Most North Hemisphere palaeoclimate records

[1]Pyrenean Institute of Ecology – CSIC, España
[2]Institute of Earth Sciences Jaume Almera (ICTJA-CSIC), España
[3]Universidad Nacional Autónoma de México (UNAM), México

Corresponding author:
Fernando Barreiro-Lostres, Department of Geo-Environmental Processes and Global Change, Pyrenean Institute of Ecology – CSIC, Campus de Aula Dei, Avda. Montañana, 1005, 50059 Zaragoza, España.
Email: ferbalos@ipe.csic.es

spanning the last two millennia include evidence of two main climate periods, although the timing is not yet well constrained (Mann et al., 2009): a warmer Medieval Climate Anomaly (MCA, 950-1250 AD; see Lamb, 1965; Hughes and Diaz, 1994) followed by a cooler Little Ice Age (LIA, 1400-1700 AD; see Bradley and Jones, 1993). However, previous reviews of these intervals have shown clear centennial-scale temperature and precipitation anomalies, and have also emphasized their spatio-temporal heterogeneity (Bradley et al., 2003; Mann et al., 2009; Diaz et al., 2011; Ahmed et al., 2013), and even an anti-phase behavior (e.g. between the western and eastern Mediterranean, Roberts et al., 2012).

A number of climate reconstructions over the last two millennia for the Mediterranean region have been recently published (see Valero-Garcés and Moreno, 2011; Moreno et al., 2012; Lionello, 2012; Roberts et al., 2012, Magny et al., 2013) which describe rapid environmental and climatic changes coinciding chronologically with the MCA and the LIA with underlying regional trends. These trends highlight timing discrepancies in palaeohydrological shifts, with associated variability in inferences concerning the definition of age ranges for wet and dry phases. In the Iberian Peninsula, numerous Late Holocene lake sequences have been analysed in a variety of geographic, climatic and ecologic settings (Julià et al., 1998; Luque & Julià, 2002; Pla & Catalan, 2005; Moreno et al., 2008, 2009; Martín-Puertas et al., 2009; López-Merino et al., 2011; Morellón et al., 2011; Corella et al., 2012; Currás et al., 2012; Höbig et al., 2012)using a variety of geological (facies, geochemistry) and biological (pollen, ostracods, diatoms, quironomids) proxies (Moreno et al., 2008, 2009; Martín-Puertas et al., 2009; Morellón et al., 2011; Corella et al., 2012; Currás et al., 2012; Höbig et al., 2012). Diatom studies have demonstrated large environmental changes in Iberian lakes during the last 2000 years in water depth, salinity and trophic status: Laguna de Medina (Reed et al., 2001), Sanabria (Luque and Julià, 2002), Enol (López-Merino et al., 2011), La Cruz (Julià et al., 1998; Kiss et al., 2007), Arreo (Corella et al., 2011), Montcortès (Scussolini et al., 2011), Estanya (Riera et al., 2004), Estany Redon (Plá and Catalán, 2005), Zoñar (Martín-Puertas et al., 2008) and Lagoa Grande (Reed, 1998; Leira, 2005). The available records show that Iberian lake dynamics responded primarily to changes in hydrology, with relatively humid conditions coinciding with the Iberian-Roman Period (IRHP, 650 BC-350 AD; Martín-Puertas et al., 2008), early Middle Ages (Dark Ages, DA, 500-900 AD; Moreno et al., 2012) and the LIA (1300-1850 AD; Morellón et al., 2011). Higher aridity usually occurs during the MCA (900-1300 AD; Moreno et al., 2012) (see reviews in Valero-Garcés and Moreno, 2011). The Iberian records show different intensities of the hydrological signatures and some asynchronies of the main changes that could be related to variable lake sensitivity and low-resolution age models, but also they suggest a regional variability in the Iberian Peninsula related to Atlantic versus Mediterranean climate impacts. Human impact in Iberian landscapes is also significant during the last two millennia (Pèlachs et al., 2009; Gil-Romera et al., 2010; Corella et al., 2013) and the climate signature in some lake records may be obscured by anthropogenic effects in the lake dynamics (Martínez-Cortizas et al., 1999; Moreno et al., 2008; López-Blanco et al., 2011; Currás et al., 2012; Roberts et al., 2011; Simonneau et al., 2013). To disentangle the complex interplay of climate and human impact during the last 2000 years and the significant regional variability in the Iberian Peninsula, more high-resolution, multiproxy and well-dated records are needed. To contribute to that effort, here we present a paleo-environmental and paleohydrological reconstruction from a detailed sedimentological, geochemical and diatom study with a robust chronological model in sediment cores obtained from the karstic Lake La Parra (Iberian Range, NE Spain).

Regional setting and study site

La Parra (39º 50' N, 1º 52' E, 1014 m a.s.l.) is one of the seven flooded sinkholes located in the complex karstic-lake system of Cañada del Hoyo, Central Iberian Range (Figure 1). This complex is developed by dissolution and fracture processes since the Pliocene (Gutiérrez Elorza and Valverde, 1994) on Jurassic and Middle to Upper Cretaceous limestone and dolostone formations (Alonso, 1986). Regional tectonic structures as the Valdemoro fault and the occurrence of a NW-SE anticlinal fold have both also played a significant role in the development of this karstic system (Eraso et al., 1979; Carmona and Bitzer, 2001).

The study site has a Mediterranean climate modulated by continental influences with large daily and seasonal temperature contrast, harsh cold winters and hot summers (from 4 ºC mean monthly temperature in January to 23 ºC in July). Annual mean rainfall is 542 mm, with July the driest month and October the wettest. Local vegetation is dominated by *Pinus nigra, Quercus faginea, Q. ilex rotundifolia, Juniperus thurifera, Buxus sempervirens* and *Q. coccifera*. Depressions and lowlands are occupied by cereal crops.

Lake La Parra has a circular morphology (113 m diameter, 1 ha surface) and steep margins (17.5 m maximum depth; Figure 1) with 10 m high vertical scarps composed of Upper Cretaceous dolomites surrounding the lake from W to SE. Influenced by a dolomite-rich watershed, the lake waters are dominated by HCO_3^- (4.78 meq/L) anions and Mg^{2+} (3.96 meq/L) cations, with pH of 8.

The lake is holomictic (Miracle et al., 1992) as shown by chemical (Electrical Conductivity from 305 µS/cm to 356 µS/cm at 16 m depth) and isotopic measurements (from -4.01 to -4.20 per mil $\delta^{18}O$, and from -38.11 to -37.46 per mil δD at surface and 16 m

water depth respectively). The lake has an ephemeral inlet and no permanent surface outlet (Carmona and Bitzer, 2001). Although no hydrological balance is available, the recent lake level fluctuations are controlled by: i) the small watershed (~ 10 ha) with reduced run-off input; ii) the low transmissivity of local and regional aquifers; iii) a high-seasonal rainfall regime with high evaporation and iv) recent use of regional aquifers by agriculture wells. The enriched $\delta^{18}O$ values in lake water (ca -4 per mil) compared to aquifer and surface waters $\delta^{18}O$ values (-8.5 to -7 per mil, Carmona and Bitzer, 2001) demonstrate a strong impact of evaporation processes in lake hydrology.

The lakes of Las Torcas karstic system are hydraulically connected to the regional carbonate aquifer and the lake levels reflect the regional groundwater levels. The main aquifer recharge area (60 % total water influx) is located in a 25 km^2 karstic area, located some 15 km north of the Las Torcas Complex. The groundwater flux is estimated as 300 l/s (Carmona and Bitzer, 2001) and follows N-S trend fractures and karstic conduits towards the south and only floods the sinkholes located topographically at <~1000 m a.s.l. From the sinkholes, groundwater drains towards the Guadazaón River fluvial aquifer.

Material and methods

In May 2010 two parallel piston cores (PA10-1A-U and PA10-1B-U) were recovered in the deepest part of the lake with the IPE-CSIC UWITEC platform and coring equipment. Later, in summer 2011, a network of 21 short gravity cores was retrieved with the UWITEC gravity corer. The piston cores were split longitudinally and photographed with the CCD camera attached to the AVAATECH X-Ray Fluorescence (XRF) scanner from the XRF-Core Scanner Laboratory of the University of Barcelona (UB, Spain). 52 samples were taken from the core PA10-1A-U for quantitative elemental geochemistry of major and trace elements by Inductively Coupled Plasma-Mass Spectrometry (ICP-MS), using a Perkin/Elmer Nexion 300X ICP-MS at the University of Pittsburgh (US-PA), following Pompeani et al. (2013). The same core was sub-sampled every 2 cm for Total Organic (TOC) and Total Inorganic (TIC) Carbon; and every 6 cm for Total Nitrogen (TN). TIC and TOC were measured with a LECO SC144DR available at the IPE-CSIC and TN with a FLASH EA 1112 LECO TRUSPEC-CN at the Centro de Edafología y Biología Aplicada del Segura (CEBAS-CSIC, Spain). Principal Component Analysis (PCA) was carried out to investigate the relationship between the chemical elements present on the sediments. Statistical treatment of the data was performed using R software (R Development Core Team, 2013). The dataset includes major elements, trace elements, and REE (determined by ICP), and also bulk geochemistry (TOC, TIC and TN). All variables were normalized with respect to their mean and standard deviation. Mineralogy was analysed every 10 cm by a Siemens D-500 X-ray diffractometer (Cu kα, 40 kV, 30 mA, graphite monocromator) at the Serveis Científico-Tècnics of the ICTJA-CSIC (Spain). Identification and relative abundance of the predominant mineralogy of the crystalline fraction were determined following Chung (1974a, b).

Sedimentary facies were described following Schnurrenberger et al. (2003). Selected samples from each facies were analysed with a JEOL JSM-6400 electron microscope coupled with an EDAX INCA 300 X-Sight for elemental identification at the University of Zaragoza (Spain).

The samples were selected considering sedimentary facies variability and therefore, the resolution varies from 20 to about 150 yr. Diatom concentration per unit weight of dry sediment was calculated following Battarbee (1986) and is expressed as valves per gram of dry sediment (v/gds $x10^6$). Relative abundances of the diatom taxa were calculated in two ways: i) based on the total diatom sum, which were used for the calculation of the planktonic and non-planktonic percentages and, ii) based on a partial diatom sum which included all species expect for *Cyclotella cyclopun*species percentages presented in figure 5 were calculated in this way. This method for expressing diatom relative abundance was chosen given the high dominance of *Cyclotella cyclopun* in the record, as excluding it from the diatom sum allows for the variations along the sequence of the non dominant species to be more evident; this explains the above 100% abundances of *C. cyclopuncta* in the diatom diagram. Taxonomic identifications and autoecological requirements for the principal diatom taxa were made using literature (Krammer and Lange-Bertalot, 1986-1991; H11). Standard extraction and counting methods (Stoermer et al. 1996) were applied to twenty samples for diatom analyses. The samples were selected considering sedimentary facies variability and therefore, the resolution varies from 20 to about 150 yr. Diatom concentration per unit weight of dry sediment was calculated following Battarbee (1986) and is expressed as valves per gram of dry sediment (v/gds $x10^6$). Relative abundances of the diatom taxa were calculated in two ways: i) based on the total diatom sum, which were used for the calculation of the planktonic and non-planktonic percentages and, ii) based on a partial diatom sum which included all species except for *Cyclotella cyclopuncta;* species percentages presented in figure 5 were calculated in this way. This method for expressing diatom relative abundance was chosen given the high dominance of *Cyclotella cyclopuncta* in the record, as excluding it from the diatom sum allows for the variations along the sequence of the non dominant species to be more evident; this explains the above 100% abundances of *C. cyclopuncta* in the diatom diagram. Taxonomic

identifications and autoecological requirements for the principal diatom taxa were made using literature (Krammer and Lange-Bertalot, 1986-1991; Håkansson and Carter, 1990; Julià et al. 1998; Håkansson, 2002; Kiss et al., 2007; Morellón et al. 2011). The dominant species in this record was identified as *Cyclotella cyclopuncta,* however this species is considered to be very close or possible conspecific with similar small centric diatoms such as *C. delicatula* or *C. distinguenda* var. *unipunctata* (see Kiss et al. 2007). The statistical treatment of the diatom dataset for Cluster Analysis was performed using the R software package (R Development Core Team 2013) together with the package ''vegan'' (Oksanen et al. 2013). Distances between clusters were recomputed by the Bray-Curtis method, using a data matrix corrected by the square root of the species percentages.The dominant species in this record was identified as *Cyclotella cyclopuncta,* however this species is considered to be very close or possible conspecific with similar small centric diatoms such as *C. delicatula* or *C. distinguenda* var. *unipunctata* (see Kiss et al. 2007). The statistical treatment of the diatom dataset for cluster analysis was performed using the R software package (R Development Core Team 2013) together with the package ''vegan'' (Oksanen et al. 2013). Distances between clusters were recomputed by the Bray-Curtis method, using a data matrix corrected by the square root of the species percentages.

To establish the chronology of the lacustrine sequence 13 AMS ^{14}C dates were obtained at the Poznan Radiocarbon Laboratory (Poland) and the DirectAMS Laboratory (US-WA) from wood fragments in long core PA10-1A-U; and ^{137}Cs and ^{210}Pb dates in short core PA-10-2A-1G, were obtained by gamma ray spectrometry at the St. Croix Watershed Research Station (US-MN). The ^{210}Pb dates were determined following Appleby (2001). The upper part of core PA10-1A-U was correlated with the short core PA-10-2A-1G using TOC values (Figure 2). Radiocarbon dates were calibrated using the curve INTCAL 09 (Reimer et al. 2009) and selecting the median of the 95.4% distribution (2σ probability interval). Age-depth model was performed with Clam code (Blaauw, 2010), adjusting the curve with a locally weighted spline.

Results

Chronological model

La Parra sedimentary sequence described in this paper is based in 11 AMS ^{14}C dates from wood samples (13 total, with two discarded reversals) (Table 1). The chronological model spans from the 3rd century AD till 2010 (Figure 2) and exhibit no apparent hard water effect. The sediment accumulation rate is rather constant throughout the record (about 4.3 mm/yr), although the deposition of some thick clastic beds (e.g. a gravel bed at 400-380 cm depth) likelyrepresent a rapid event. ^{210}Pb/^{137}Cs inferred accumulation rates are as well rather constant during mid 1800–mid 1900 (0.03-0.1 g/cm^2/yr^{-1}), however increased since 1970s up to 0.2 g/cm^2/yr^{-1}. ^{210}Pb dating is considerably less accurate below 25 cm, therefore the time resolution decreases prior to 1900. The ^{137}Cs profile shows a gradual pattern rather than having a sharp peak, as consequence of some post-depositional diffusion of ^{137}Cs. However, the broad ^{137}Cs peak provides additional support for the ^{210}Pb dating and the ^{14}C-based chronology.

Sedimentary Facies and Units

Sedimentological description of surface sediments obtained from 21 short cores allows three main lacustrine environments to be defined across the basin (Barreiro-Lostres, 2012): i) an external-littoral platform up to 2 m water depth, with aquatic vegetation stabilizing the substrate, deposition of coarse sand and silt sediments (facies 2.2 and 1.3 respectively; see Table 2) and with the presence of active gravity processes as rock falls, where rocks are detached from the northern vertical margin of the doline; ii) an internal-littoral to profundal-distal zone with a steep and narrow talus (2-10 m depth) with brown and grey coarse to fine silts (facies 1.3 and 1.1); and iii) a profundal-distal zone (10-16m depth, 80 m wide) with deposition of banded grey silts grading to black, more organic silts in the deeper central areas (facies 1.1, 16-17 m depth).

The La Parra long core (PA10-1A-U) reached the Cenomanian greenish marl substrate and so the whole lacustrine sequence deposited in the doline was recovered (Figure 1). The marl substrate (facies 5, see Table 2) shows evidences of carbonate dissolution, brecciation and alteration and clay enrichment, common in carbonate substrate after a prolonged period of karstification (Gutiérrez et al., 2008). The La Parra sedimentary sequence is mostly composed of clastic carbonate facies ranging from gravels (see Table 2, facies 3); fine and medium-coarse sands (facies 2.1 and 2.3 respectively); fine, medium and coarse silts (facies 1.1, 1.2 and 1.3 respectively); to finely laminated silts (facies 4). They are organized in fining-upward sequences from 10 to 60 cm thick. This great facies variability is notorious for a relatively small karstic lake (Table 2). Clastic carbonates are common in Iberian karst lakes and they reflect deposition in littoral (coarse facies) to distal (fine facies) settings influenced by variable lacustrine reworking and alluvial processes (see review by Valero-Garcés et al., 2014). Deposition in La Parra Lake is controlled by the carbonate nature of the watershed (source area), the varied intensity of the sediment delivery processes (run-off and creek activity) and the changing limnological conditions (water depth, organic productivity, bottom redox conditions). Although lake level fluctuations are difficult to quantify from clastic facies sequences, grain size and texture provide some constrains for

depositional depths. So, the short-core survey shows that massive to banded silts are common lacustrine facies in sublittoral to more profundal settings. Finely laminated facies (facies 4) in these karst lakes only appear when anoxic environments dominate the lake bottom, often associated with higher lake levels and/or limnological conditions conducive to more frequent water stratification (Julià et al., 1998; Romero-Viana et al., 2009a; López-Blanco et al., 2011; Valero-Garcés et al., 2014). The occurrence of gravels (facies 3) and coarse sands (facies 2.3) in the central areas of La Parra Lake indicates periods of increased erosion and runoff during likely lower lake levels.

Carbonate minerals (dolomite and calcite) are the main sediment component, and rather constant along the sequence (80-90 % mean). They are mostly of detrital origin, eroded from the Cretaceous carbonatic rocks in the watershed and transported by the small creek entering the lake at the SW margin. Endogenic minerals (calcite as main component and secondarily aragonite and high-magnesium calcite) appear in five discrete intervals, either in fine laminated facies due to the in-lake calcite precipitation or in coarser sandy and gravel facies, likely due to reworking of older lacustrine sediments. Laminated facies (facies 4, see Table 2) contain both white laminae made up of 3-5 µm calcite crystals and dark laminae composed of amorphous organic matter and silicates, similar to those found in other karstic lakes of the Iberian Peninsula (La Cruz, Romero-Viana et al., 2008; Zoñar, Martín-Puertas et al., 2008; Montcortès, Corella et al., 2010;Arreo, Corella et al., 2011), and interpreted as seasonal deposition of calcite precipitated in the epilimnion in summer during the climax of algal development (white laminae) and clastic material deposited during autumn-winter (dark laminae). This lamination is associated with low energy sedimentation environments, favoured by water stratification during high lake levels and prone to anoxic redox conditions in the bottom (Brauer et al., 2004).

From the bottom to the top, seven sedimentological units (VII to I, Figure 3) have been characterized. The units are defined by the occurrence of distinctive facies and the boundaries are set at abrupt changes at the base of fining upward sequences. The basal Unit VII (640-620 cm) is bounded by the Cretaceous basement at the bottom and the onset of banded grey silts at the top. It is comprised of a mixture of decalcified silty matrix (see Table 2, facies 5; >90% clay minerals and quartz) and large carbonate clasts (1-5 cm of diameter) with irregular and angular morphologies. Unit VI (620-570 cm) is composed of medium to coarse banded silts (see Table 2, facies 1.2 and 2.2) and finely laminated silts (facies 4) with presence of endogenic carbonates (calcite and secondly aragonite and high-magnesium calcite). This unit represents the onset of lacustrine sedimentation and the upper boundary is set in the first occurrence of sandy facies. Unit V (570-400 cm) started with a 60 cm thick fining upward sequence comprised of fine and coarse (see Table 2, facies 2.1 and 2.2 respectively) and medium silt (facies 1.2); following with deposition of five fining upward sequences (darker coarse-medium silts, facies 1.2 and 1.3). Unit IV (400-250 cm) is separated from Unit V by the presence of a unique 20 cm thick coarse gravel layer at 400 cm (facies 3). Unit IV is composed of three fining upward sequences of alternating medium to coarse silts (facies 1.2 and 1.3 respectively) in layers with irregular, erosive bases. The base of Unit III (250–95 cm) is set at a coarse sandy interval (facies 2.2); the occurrence of fine laminated sediments with endogenic carbonates (calcite + aragonite + high-magnesium calcite; facies 4) singles out this unit. Internally it is composed of seven fining upward sequences including coarse silts (facies 1.3, 15 cm mean thick intervals) and fine-laminated silts (facies 4, in ca. 5 cm thick sets), with punctual intercalation of coarse sands (facies 2.2, 5 cm thick). Unit II (95-40 cm) is composed of coarse banded silts (facies 1.3) with high TOC/TN values deposited after a thin coarse sandy interval (facies 2.2) at the base. Unit I (40-0 cm) is characterized by deposition of fine-medium dark grey silts (facies 1.1 to 1.2) topped by coarse dark silts (facies 1.3), with low TOC/TN values. Most units (V, IV, III and II) show a general fining upward trend, and within each unit, sediments are also organized in fining upward sub-sequences (sand-silt or coarse-fine silts). The only coarsening upwards sequence occurs in Unit VI.

Geochemistry

Total Inorganic Carbon (TIC) values along the sequence show a slight variability around mean values of 6%, with the lowest values at the base of the core and the highest values associated with fine laminated facies (Figure 3). TOC content follows a similar trend to TIC (~3% mean) with the highest values in finely laminated facies (6-7%) and towards the top Unit I (4.5%). TOC/TN atomic ratios show large variability (3-40). The highest values (40) are located at the base of the sequence (Unit VII) and towards the the top of unit III and in unit II. Geochemical composition is driven by the detrital nature of the sediments. Ca/Ti and Sr/Ti ratios present relatively low values along the Units VI and V, except at the bottom of Unit V (560 cm), and a slightly increasing trend in Unit IV. Ca/Ti and Sr/Ti ratios show peak values in Unit III during the deposition of finely laminated silts and in recent times (Unit I). Ti, Pb and Fe values follow a similar trend on the whole sequence, with distinctive peaks at 470 cm (Unit V), 310 cm (Unit IV) and an increasing trend from 250 cm (start of Unit III) towards the top of Unit I (Figure 3).

The principal component analysis (PCA, Figure 4) of the geochemical dataset including ICP and LECO results shows that the first two components explain

48% of the total variance of the dataset (26% the first eigenvector and 22% the second). The remaining PCA components explain variance percentages <12% and they have not been taken into account. Negative values of the first principal component (PC1) are related to elements associated with clastic input (Fe, Ti, Pb, Si, Al) and with high TOC/TN values suggesting that terrestrial organic matter (plant macrofossils and soil organic matter, see Meyers and Lallier-Vergés, 1999) enters the lake with the terrigenous material. PC1 and detrital mineral (dolomite + quartz + clay minerals) profiles show similar patterns. The second principal component (PC2) is related to chemical elements associated with in-lake biological and endogenic carbonate productivity, such as Ca, Sr, TOC and TIC (Figure 4). The plot of PC1 with respect to the sample core depth highlights three short intervals of higher clastic input (negative values) to the lake in units V, IV and III (ca. 550, 1000 and 1500 AD) and a longer interval in Units II and I (1600–1950 AD). After 1950 AD, PC1 values slightly decreased. On the other hand, the plot of PC2 values with respect to their core depth indicates that higher in-lake carbonatic and organic productivity (positive values) occurred in three main intervals coinciding with relatively lower clastic input to the lake and with the sedimentation of fine laminated facies with endogenic carbonates - transition from Unit VI to Unit V (380-450 AD), top of Unit IV and Unit III (1150-1600 AD) - and in Unit I (after 1950 AD).

Diatoms

Diatom preservation is good along the record except for the samples from sandy intervals –e.g. 440 cm, 660 AD; 199 cm, 1339 AD-. In total, 43 diatoms species were identified, dominated by planktonic species (82-96 %), amongst which *Cyclotella cyclopuncta* is the most abundant taxa followed by *C. distinguenda*, a species indicative of higher alkalinity (Krammer & Lange Bertalot 1991). Diatom zonation based on cluster analyses identifies four major zones with boundaries which coincide with the limits between lithostratigraphic units. Given the lower resolution of the diatom record its zones tend to be broader compared with lithostratigraphic units: diatoms zone 1 includes units I and II; zones 2 and 3 correspond to unit III and IV respectively, and zone 4 includes units V and VI (Figure 5) The bottom of diatom zone 4 (unit VI) has relatively high diatom abundance with high proportions of *C. distinguenda* and the presence of *D. stelligera*. At the top of zone 4 (Unit V) diatom concentration and *C. cyclopuncta* abundance have their lowest values while *C. distinguenda* and non-planktonic diatoms *(N. diluviana*) are the most abundant. In zone 3 (Unit IV) there is a recovery in diatom concentration, again dominated by *C. cyclopuncta* and *C. distinguenda.* The highest diatom concentration is in zone 2 (Unit III), which also shows maximum values of *C. cyclopuncta*, and minimum of *C. distinguenda.* This zone also has high abundance of non-planktonic taxa such as *A._minutissimum, E. microcephala* and *E. cesatii.* In zone 1 (Units II and I) *C. distinguenda* increases in abundance again, with persistent high values of *C. cyclopuncta*; the most recent sample is characterized by an increase in *D. stelligera* and in total diatom abundanc*Diatoms*

Diatom preservation is good along the record except for the samples from sandy intervals –e.g. 440 cm (660 AD) and 199 cm (1339 AD)-. In total, 43 diatoms species were identified, dominated by planktonic species (82-96 %), amongst which *Cyclotella cyclopuncta* is the most abundant taxa followed by *C. distinguenda*, a species indicative of higher alkalinity (Krammer & Lange Bertalot 1991). Diatom zonation based on cluster analyses identifies four major zones with boundaries that coincide with the limits between lithostratigraphic units. Given the lower resolution of the diatom record its zones tend to be broader compared with lithostratigraphic units: diatoms zone 1 includes units I and II; zones 2 and 3 correspond to unit III and IV respectively, and zone 4 includes units V and VI (Figure 5).
The bottom of diatom zone 4 (unit VI) has relatively high diatom abundance with high proportions of *C. distinguenda* and the presence of *Discostella stelligera*. At the top of zone 4 (Unit V) diatom concentration and *C. cyclopuncta* abundance have their lowest values while *C. distinguenda* and non-planktonic diatoms *(Navicula diluviana*) are the most abundant. In zone 3 (Unit IV) there is a recovery in diatom concentration, again dominated by *C. cyclopuncta* and *C. distinguenda.* The highest diatom concentration is in zone 2 (Unit III), which also shows maximum values of *C. cyclopuncta*, and minimum of *C. distinguenda.* This zone also has high abundance of non-planktonic taxa such as *A. minutissimum, Encyonopsis microcephala* and *E. cesatii.* In zone 1 (Units II and I) *C. distinguenda* increases in abundance again, with persistent high values of *C. cyclopuncta*; the most recent sample is characterized by an increase in *D. stelligera* and in total diatom abundance.

Discussion

Depositional Evolution of La Parra

The decalcified sediments of the base of La Parra sequence (Unit VII, 640–620 cm) represent the top of the karstified Cretaceous substrate. Prior to 300 AD the sinkhole drained to the aquifer and the bottom was subaerially exposed. High and increasing TOC/TN ratio values in this interval reflect high terrestrial organic mater content, likely related to soil-forming processes at the bottom of the sinkhole (Figure 6).

Deposition of brown fine silts with higher TOC, TIC and increasing Ca/Ti and Sr/Ti values (Unit VI, 620–570 cm, 340-400 AD) represent the early flooding of

the sinkhole with raising groundwater levels (figures 3 and 6). The low clay mineral content and higher PC1 values mark reduced sediment input to the sinkhole; the low PC2 scores indicate low endogenic carbonate productivity during this early lake flooding stage. High diatom concentration and predominance of planktonic taxa (*C. cyclopuncta* and *C. distinguenda*) suggests the doline flooded quickly and reached relatively high water levels soon. At the same time, the high abundance of *D. stelligera* suggests relatively high nutrient availability (Köster and Pienitz, 2006), and may be related with remobilization of nutrients accumulated in the flooded soils. ???) may be related with remobilization of nutrients accumulated in the flooded soilsThe early deposition of finely-laminated silts with precipitation of endogenic carbonates at 600 cm (350 AD), which is favored by water stratification during high lake levels as documented in the nearby Lake La Cruz (Romero-Viana et al., 2008), also points to rapid lake level increase during the early phase of lake development.

The occurrence of coarse sands in the centre of the lake underlines the drastic limnological change at the onset of Unit V (570–400 cm, 400-750 AD). PC1, as a geochemical indicator for watershed erosion and sediment delivery, shows a centennial increasing–decreasing trend along this unit. It peaked ca. 600 AD (Figure 6) and decreased afterwards suggesting a reduction of soil erosion, coherent with lower human pressure after the Visigoth decline (last half of 7th century AD) and during the Moorish period (8th-11th century AD) (Burjachs, 1996; López-Blanco et al., 2011). Fe and Ti profiles track the fining upward sequences and demonstrate the significant alluvial influence in the lake sedimentation during Unit V when diatom abundance is the lowest in the sequence maybe due to a dilution effect caused by the high clastic sediment input. The maximum *N. diluviana* and chrysophyte cysts values correspond with a decrease in the dominant *C. cyclopuncta* (planktonic), suggesting a shallower lake stage up to 500 cm (ca 550 AD). The decrease in non-planktonic species is coherent with a lake levels recovery during deposition of finer facies towards the top of the unit. Unit V, when diatom abundance is the lowest in the sequence may be due to a dilution effect caused by the high clastic sediment input. The maximum *N. diluviana* and chrysophyte cysts values correspond with a decrease in the dominant *C. cyclopuncta* (planktonic), suggesting a shallower lake stage up to 500 cm (ca 550 AD). The decrease in non-planktonic species is coherent with a lake levels recovery during deposition of finer facies towards the top of the unit. Carbonate and biological productivity along unit V is generally low (low Ca/Ti, Sr/Ti ratios and TOC values, low diatom abundance).

Unit IV (400–250 cm, 750-1150 AD) starts with deposition of the only gravel bed (400-380 cm) in the sequence. Both, high alluvial input and lower lake levels are main factors favoring sedimentation of coarse sediments in the deepest areas of the sinkhole. Although detrital minerals (dolomite, quartz and feldspars and clays) content is still high, geochemical indicators (PC1) continued with the decreasing trend initiated in the previous unit during the first three fining upward sequences (400–320 cm, 750-950 AD). A second peak in sediment delivery and watershed erosion occurred at 320-280 cm (950-1050 AD) as shown geochemical indicators (PC1, Figures 3 and 6). The abundance of *C. distinguenda* indicates persistence of relatively alkaline water.The abundance of *C. distinguenda* indicates persistence of relatively alkaline water.

Unit III (250-95 cm, 1150-1630 AD) is characterized by the presence of finely laminated silts composed of endogenic carbonatic minerals. It presents the highest values of Ca/Ti, Sr/Ti ratios and TOC (~6%), the highest diatom abundance and the lowest values of TOC/TN (~9) of the record (Figure 3). All of these indicators point to a period with the highest carbonate and biological productivity of the sequence. Diatom communities are diverse, dominated by planktonic *C. cyclopuncta* and non-planktonic *Encyonopsis* and *Achnanthidium* species; *C. distinguenda* shows minimum values, suggesting less alkaline waters, probably related with higher lake levels. Diatom communities are diverse, dominated by planktonic *C. cyclopuncta* and non-planktonic *Encyonopsis* and *Achnanthidium* species; *C. distinguenda* shows minimum values, suggesting less alkaline waters, probably related with higher lake levels. The relatively higher abundance of benthic species during these laminated intervals may reflect the expansion of littoral environments caused by the rise of lake levels, the transport and reworking of benthic littoral diatoms as suggested by the occurrence of sandy layers intercalated within the fine laminated facies, or the high variability of lake level at annual/decadal scales during this period. Some thin gravel and sand layers occurred at the top of unit III, paralleling an increase in TOC/TN, detrital minerals and a PC1 peak.

The absence of laminated facies and the return to deposition of alternating light and dark grey silts marks the onset of Unit II (95–40 cm, 1630–1850 AD). This unit presents the highest TOC/TN (~40) values of the sequence and relatively lower TOC and diatom abundance. PC2 sharply decreased, pointing to less biological and endogenous carbonate productivity. Lower but increasing PC1 scores mark a third period of intense watershed erosion, starting around 1600 AD and lasting until the top of the unit (ca. 1850 AD, Figure 6).

The top Unit I (40–0 cm, 1850-2010 AD) is characterized by deposition of dark grey silts with higher TOC, significantly lower TOC/TN ratios, and an increasing trend in endogenic carbonates content. Sediment delivery to the lake as indicated by the dominance of finer silts facies and the PC1 values continued to be generally higher during the last

century. However, significant changes in carbonate and organic productivity occurred. TOC values show three main periods: < 1.5 % between 40-28 cm (1850 - 1908 AD); an increase up to 3.5 % until 15 cm, (1908 -1966 AD) and higher than > 3.5 % during the top 15 cm (last 44 years) (Figures 2 and 3). This general increase in TOC is paralleled by a decrease in TOC/TN and reflects an increase in endogenic bioproductivity, while the reappearance of *D. stelligera* suggests nutrient-enriched water and some level of eutrophication. Compared to the 19th century, detrital and allochtonous organic material input decreased rapidly (low dolomite and silicate % and low TOC/TN values) parallel to an increase in bioproductivity during the early and mid 20th century (1920s till 1970, 23-13 cm). The decrease in soil erosion (lower TOC/TN) and the increase in carbonatic and organic productivity in the lake could be a reflection of the population decrease during the 20th century caused by the rural exodus from villages to cities and the abandonment of crop fields with the consequent decrease of anthropogenic disturbance. However, after the 1970s (top 13 cm), sediment accumulation in the lake rapidly increased from 0.05 to 0.2 gcm^{-2} yr^{-1} (Figure 2), although TOC continued increasing and TOC/TN remained low. Coarser sedimentation during the last 30 years in La Parra could imply a slight lowering of water levels accompanied by higher anthropogenic disturbance in the area. These trends point to a recent change in the lake dynamics that could be caused by increasing human pressure due to tourism.

Cañada del Hoyo hydrological and environmental changes for the last 1600 years

Lake records spanning the last millennium are available from three lakes of the Cañada del Hoyo karstic system (Figure1): La Cruz (Burjachs, 1996; Julià et al., 1998; Rodrigo et al. 2001; Romero-Viana et al., 2008, 2009a, 2011); Lagunillo del Tejo (Romero-Viana et al., 2009b; López-Blanco et al., 2011) and La Parra (this study). Although chronological models do not have similar resolution (Figure 1), and the proxies used to reconstruct lake level and environmental changes differ from one another, the proximity of these lakes provide an opportunity to evaluate the regional significance of reconstructed hydrological/environmental changes in a context of similar climate forcing and human impact. Therefore, differences in climate forcing and human impact can be discounted in interpreting these environmental records. Furthermore, this study shows how some particular lake features may control the sensitivity of the system to record past changes. The ^{14}C age model for Lake La Parra is the most robust of the three sites: 11 ^{14}C AMS dates versus 1 for Lake La Cruz and 5 for El Lagunillo.

Palaeohydrological changes. The main episodes of hydrological change during the ca. 300 to 2010 AD period defined in lake La Parra (Figure 3) should be reflected in all Las Torcas complex (Figure 6). The most arid phase of the last 2 millennia, represented by Unit VII, occurred before ca. 300 AD, when the sinkhole was dry. The length of this period of subaerial exposure and vertical drainage in the sinkhole is unknown, but it was long enough to produce intense karstic decalcification processes and the alteration of the Cretaceous substrate. The flooding of the doline (Unit VI) at about 300 AD inaugurated a generally more humid period during the last 1.6 ka with highly fluctuating lake levels but without another drying out phase. Two main transitions occurred at 1200 and 1600 AD defining three main stages: i) intermediate but fluctuating lake levels occurred during the 400-1200 AD period (Units V and IV), with the lowest during 750-850 AD; ii) the highest lake levels occurred during 1200–1600 AD (Unit III), and iii) since 1600 (Units II and I) lake level remained lower than during the 1200-1600 AD period, although higher than before 1200 AD.

The rapid change in the hydrological behavior of La Parra sinkhole at about 300 AD (Figure 6, Unit VII) is a conspicuous feature. Rainfall and subsequent changes in aquifer-recharge and local groundwater flows play an important role in recent lake level changes (Carmona and Bitzer, 2001; unpublished data from Water Agency of Castilla-La Mancha Autonomous Community). At longer time scales, in this non-active tectonic area, other factors besides climate (changes in karst dynamics, local base level) could have been conducive to the flooding of the sinkhole. Although the complete lake sediment sequences has not been recovered in any of the other Cañada del Hoyo lakes, the available data suggest they do not span more than a few millennia. The recovered La Cruz record spans the last ca. 1500 years and efforts to retrieve longer cores were encountered with a hard surface that might be interpreted as the Cretaceous substrate (Burjachs et al., 1996). The base of the sequence recovered in the nearby lake El Tejo in 2012 (Figure 1C, study in progress) is composed of coarse sands, suggesting littoral sedimentation and has been dated as 3200 ± 66 cal ^{14}C yr BP. Changes in the base level of the Guadazaón River could also have had an impact on groundwater and sinkhole lake levels. Higher fluvial incision prior to 300 AD could explain desiccation of the sinkholes but there is no geomorphologic evidence of such a river dynamic change during the 4th century AD (Gutiérrez Elorza and Valverde, 1994). As a whole, the available data support an increase in precipitation as the main reason for a rapid flooding of La Parra ca. 300 AD.

Sedimentological and geochemical indicators show a multi-decadal variability in lake level during 400–750 AD (Unit V). The deposition of the thickest gravel bed of the record (around 750 AD, Figure 6) marks a large depositional change in La Parra: coarse

sedimentation reached the center of the lake during an episode of increased run-off and lower lake level. This episode coincide with three important droughts between 748-879 AD documented in Al-Andalus by contemporaneous Moorish historians (Domínguez-Castro et al., 2014). Once lake level recovered, during the next ca 400 years (AD 800–1200, Unit IV) only three major fining-upward sequences occurred. Later, the deposition of fine-laminated silts and the rapid increase in carbonate endogenic minerals content (the highest of the sequence) mark the transition towards a long period (1200–1600 AD, Unit III) characterized by higher lake levels in La Parra, with frequent anoxic conditions, and higher biological activity leading to more endogenic calcite formation. Up to seven finely laminated facies intervals with endogenic calcite (Ca/Ti and Sr/Ti peaks) occurred between 1200-1600 AD (Figure 6). They reflect decade-long periods of higher lake levels, and likely higher winter precipitation. In lake La Cruz and Lagunillo del Tejo (Julià et al., 1998; López-Blanco et al., 2011), more frequent anoxic conditions also occurred during the last centuries, but the onset is different and occurred generally later than in La Parra. In La Cruz, deposition of finely laminated facies indicative of meromictic conditions only started after 1700 AD but continued till recent times (Julià et al., 1998). In Lagunillo del Tejo, better laminated, more organic facies occurred during several intervals (1100-1150, 1250-1550, 1650-1800 and 1950-2000 AD). Fine laminated silts in El Tejo (Figure 1C) only occurred at the top of the sequence, after ca. 1600 AD. Development of meromictic conditions on these karstic lakes is related to the synergetic effects of climatic (higher winter precipitation, colder temperatures, weaker winds), hydrological (higher lake levels), and anthropic forcings (land-cover changes, nutrient and sediment input).

Human impact and lake dynamics

The main periods of human impact in La Parra watershed as indicated by PC1 values (Figure 3) occurred at the end of the Visigoth Period and the early Moorish Period (ca 500–700 AD), at around ca 1000 AD, 1450-1500 AD, 1550-1650 AD and since 1700 AD till recent times. The increase in sediment delivery during the interval 950-1050 AD correlates with the Muslim and Christian wars when burning forest was a common military strategy (Burjachs et al., 1996). Deposition of the last thick sandy layer in the sequence at around 1200 AD (Unit III) could also reflect higher landscape transformation around the time of the Christian conquest of Cuenca (1177 AD).

The other two lake records from Las Torcas also show higher human activities in the watersheds during medieval times. Human impact in the watershed was mainly due to transhumance practices that peaked during the XVth-XVIth centuries (highest cattle heads around 1526 AD), deliberate fires and deforestation for grazing and farming (Burjachs, 1996; Julià et al., 1998; Romero-Viana et al., 2008; López-Blanco et al., 2011). In Lagunillo del Tejo three peaks of microscopic charcoal occurred during the 1200-1600 AD period indicative of higher human pressure in the landscape (López-Blanco et al., 2011; Figure 6). Pollen record from La Cruz confirms the more intense use of the land during the Medieval times (Burjachs et al., 1996).

The return to massive silt deposition with coarser silt intervals and the highest TOC/TN ratios of the sequence in La Parra point to intensified erosion in the lake's basin, higher input of allochtonous sediments and terrestrial organic matter, and relatively shallower water levels during the 1550–1650 AD. High scores of PC1 suggest another peak of large human impact between 1800-1850 AD (50-40 cm) that corresponds with higher population and also a period of Civil wars and significant land use changes related to new confiscation laws, changing from livestock to intensive agricultural practices (Lozano-Sahuquillo, 2002; López-Blanco et al., 2011). The maintained increase in watershed erosion and sediment delivery to the lake along 19th–20th centuries occurred during the period of increasing population in Cañada del Hoyo village and agriculture expansion in the lakes area (López-Blanco et al., 2011). A large macrocharcoal peak in Lagunillo del Tejo also occurred at this time (Figure 6; see López-Blanco et al., 2011).

Interestingly, each lake in the Cañada del Hoyo complex might record a different evolution during this period of the highest human pressure in the region. Some of the differences may be due to the age model uncertainties and the varied sensibility of the proxies used for each paleoenvironmental reconstruction. However, watershed topography, bathymetry and land uses seem to play a definitive role in each lake basin. In Lagunillo del Tejo, lake levels dropped and erosion increased due to the construction of agricultural terraces within the lake basin (Romero-Viana et al., 2009b; López-Blanco et al., 2011). Lake La Cruz maintained a high water-level with varves sedimentation until present day (Julià et al., 1998). In La Parra, sediment delivery (PC1) remained high and bioproductivity as indicated by PC2 and diatom abundance remained low. Human impact was larger in Lagunillo del Tejo than in La Cruz and La Parra because of the topographic configuration of the watershed (more available flat areas for farming) and its shallower nature (< 7 m compared to 17 in La Parra and 25 in La Cruz).

Timing of paleohydrological changes in the Iberian Peninsula

The main paleohydrological changes identified in Las Torcas sequences have been documented in most Iberian records, but the timing shows noticeable differences.

The pre-300 AD arid period has also been detected in another Iberian Range karstic lake (Somolinos Lake, Currás et al., 2012). Interestingly, Lake La Parra was a dry sinkhole during much of the Iberian-Roman Humid Period (650 BC-350 AD, following Martín-Puertas et al., 2008) characterized as the most humid period in southern Spain during the last 4 ka. Although the relatively arid phase around 100 AD detected in Zoñar Lake could be correlated with La Parra arid phase, available records suggest that the Roman Period was wetter in the South than in central (Somolinos Lake, Torcas complex) and northern (Lake Arreo, Corella et al., 2013; Lake Moncortés, Corella et al., 2010; Lake Estanya, Morellón et al., 2008) Iberian Peninsula. As a whole, in the Iberian Peninsula more humid conditions prevailed during the early Iberian–Roman Humid Period (IRHP, 500-0 BC), and the climate became more arid towards the end of the Roman Period (100 BC–350 AD) (Gutiérrez-Elorza and Peña-Monné, 1998; Martín-Puertas et al., 2008; Currás et al., 2012; Pérez-Lambán, 2013), although with high variability in terms of timing and intensity (Corella et al., 2013).

Lower lake levels, evidences of increased aridity and a decrease of flood intensity and frequency have been documented all over the Iberian Peninsula somehow synchronous to the Medieval Climate Anomaly (MCA), from 900 AD to 1300 AD (following Moreno et al., 2012): in the South (Zoñar Lake, Martín-Puertas et al., 2008), in the Iberian Range (La Cruz Lake, Julià et al., 1998; Taravilla Lake, Moreno et al., 2008; Lagunillo del Tejo, López-Blanco et al., 2011), in the Central System (López-Sáez et al., in press, Somolinos Lake, Currás et al., 2012) and in the Pyrenees (Lake Redon, Pla and Catalán., 2005; Lake Montcortés, Corella et al., 2012; Lake Estanya, Morellón et al., 2011). The onset of this drier period is not synchronous all over the Iberian Peninsula, and, a prior phase of low lake levels *ca* 750–850 AD has been documented in Central (La Parra; this study; Somolinos Lake, Currás et al., 2012; Taravilla Lake, Moreno et al., 2008) and Northern Spain (Lake Arreo, Corella et al., 2013). However, antiphasic hydrological conditions during the MCA are indicated in records from NW Iberian Peninsula, influenced by the Atlantic Ocean, relative to those from the South and Northeast, where a Mediterranean influence predominated (Lebreiro et al., 2006; Moreno et al., 2008). Despite local differences and some chronological inconsistencies, the Iberian sequences present a clear evidence that the MCA (900-1300 AD) was a dry period in the Mediterranean Iberian Peninsula, with decreased lake levels, more xerophytic and heliophytic vegetation, a low frequency of floods, major Saharan aeolian fluxes, and less fluvial input to marine basins (Moreno et al., 2012).

The first evidence for wetter conditions and higher lake levels after the MCA occurred almost at same time (~1200 AD) in La Parra and Zoñar, that is around 100 years before than in Northern Spain (Lake Arreo, Lake Montcortés, Lake Estanya, Lake Redon). Relatively more humid conditions lasted only for 400 years (1200-1600 AD) in central and southern Iberia, while in the North continued until 1900 AD. In La Parra, this wetter period is composed at least by seven hydrological oscillations, implying multi-decadal changes from 1200 to 1600 AD. Some of these fluctuations were severe enough to result in gravel deposition (ca. 1550 AD). An increase in winter rainfall has been interpreted by documentary sources (Rodrigo and Barriendos, 2008) for Andalusia (southern Spain) for the last decades of the 16th century and the first half of the 17th century, as well as an increase in the frequency of the floods in the Tagus river basin from 1590 to 1640 (Benito et al., 2003), and a general increase of floods in Taravilla Lake (Central Spain, Moreno et al., 2008). Dendroclimatic studies (Creus Novau, 2000; Saz-Sánchez, 2003) also found rainfall anomalies prevailed over thermal anomalies during the LIA in Spain. The tree ring index shows a rainfall maximum during the second half of the 16th century, general dry conditions in the 18th century, and a recovering of rainfall in the mid-19th century. Reconstructed rainfalls during the LIA from documentary data (Rodrigo and Barriendos, 2008) identified clear differences among Mediterranean locations showing a wide hydrological N-S variability in the Iberian Peninsula also pointed by other authors (Martínez-Cortizas et al., 1999; Domínguez-Castro et al., 2008; Fletcher and Zielhofer, 2013).

The change towards drier conditions in Lake La Parra at the end of the LIA (about 1600 AD) occurred about 200 years earlier than other northern Iberian lakes (about 1800 AD). These drier conditions are in good agreement with the documentary sources in Andalucía (Rodrigo and Barriendos, 2008) and the low frequency of paleofloods in the Tagus River (Benito et al., 2003) and Taravilla lake (Moreno et al., 2008) during the XVII-XIX centuries. Although sedimentological and geochemical evidence suggest that lake levels in La Parra during the 20th century remained relatively constant, several lakes in Central (Lagunillo del Tejo), South (Lake Zoñar) and North Spain (Lake Estanya) have shown lower lake levels after the end of the LIA and during the early 20th century.

Mediterranean variability

La Parra main hydrological climatic-related changes are in agreement with the main West (Ahmed et al., 2013; Magny et al., 2013; Nieto-Moreno et al., 2011, 2013; Lebreiro et al., 2006) and Central Mediterranean (Magny et al., 2013) climate reconstructions, although most available lacustrine records from these regions lack of enough temporal resolution during the last 2000 years to establish reliable comparisons (Jones et al., 2009).

The wetter conditions in Lake La Parra at the end of

the IRHP (350 AD) match with more humid conditions in the Alborán Sea (Nieto-Moreno et al., 2011) and an increase in flooding events described in North Italy sites (Lake Ledro, Wirth et al., 2013, Lake Accesa, Magny et al., 2013), as well as high lake levels (Magny et al., 2013). The drier (more humid) nature of the MCA (LIA) correlates well with an increase (decrease) in aridity interpreted by the Alborán records, linked with a decrease (increase) of flooding events in Lake Ledro. Although the MCA and LIA climatic phases from West and Central Mediterranean correlate well with Iberian records, despite minor local variability and some chronological differences, it is worth noticing that main hydrological changes occurred earlier in La Parra than elsewhere. La Parra suggests that the last part of the Dark Ages (500-900 AD) was already showing an aridity signature and that the MCA ended around 1200 AD, earlier than in northern Europe. The early onset of the more humid LIA around 1200 AD is in agreement with an increase in flooding events in the southern Alps (Lake Ledro, Wirth et al., 2013) during the 1200-1300 AD. These differences in timing detected in La Parra record and correlated to other regional sequences point to a singular hydrological response of the western Mediterranean areas during the last millennia to climate variability.

On the contrary, La Parra record shows an opposite hydrological pattern compared with East Mediterranean sites, as Nar Gölü (Jones et al., 2006) and the Dead Sea (Neuman et al., 2007), and supports the hypothesis (Roberts et al., 2012) of an East–West Mediterranean paleohydrological see-saw during the last 2 millennia (Figure 6). This anti-phase pattern between western and eastern Mediterranean records has been explained by atmospheric teleconnections between the North Sea and the Caspian Sea (Jones et al., 2006) and demonstrates that the LIA/MCA hydroclimatic pattern in the Mediterranean was determined by a combination of different climate modes (including NAO forcing) along with major physical geographical controls.

The main hydrological and climatic changes identified in lake La Parra coincide with two Holocene rapid climate changes (RCCs) described by Mayewski et al. (2004) during the last millennium (800-1000 AD and 1400-1850 AD) and with global model simulations (Mann et al., 2009; Wanner et al., 2008), with a dry and warm Medieval Climate Anomaly (950-1250 AD, following Mann et al., 2009) and a wet and cold Little Ice Age (1400-1700 AD, following Mann et al., 2009). The Iberian Roman Humid Period (650 BC-350 AD; Martín-Puertas et al., 2008) identified in La Parra and other Mediterranean areas does not correspond to a global RCC. The period of relatively lower lake levels and increased sediment delivery to the lake in La Parra (400-1200 AD, and especially 750-850 AD) falls within the 800-1000 AD RCC interval at hemispheric scale due to southward migration of the Inter-Tropical Convergence Zone (Mayewski et al., 2004). Hydrological changes during the MCA and the LIA are consistent with a NAO–like dynamics at centennial scales (Trouet et al., 2009; Nieto-Moreno et al., 2011; Roberts et al., 2012) and changes in solar centennial-scale irradiance (Wanner et al., 2008; Lebreiro et al., 2006). A mechanism relating phases of decline in solar output and more frequent negative modes of the North Atlantic Oscillation (NAO) - thus reducing North-South pressure gradient over the North Atlantic and shifting the Westerlies to a southerly position - has been postulated to explain positive precipitation anomalies in the north-western Mediterranean area during the LIA (Xoplaki et al., 2004; Moreno et al., 2008; Nieto-Moreno et al., 2011). Nevertheless, the reconstructions do not show a univocal north-south trend in Iberian lakes, as proposed by Magny et al., (2013; 2012) for the Italian Peninsula, with clear latitudinal changes at latitudes about 40 N.

Conclusions

The sedimentary record of Lake La Parra demonstrates the high sensitivity to hydrological changes of small sinkholes and the rapid response to human induced land use changes in the watershed. The main periods of human impact in the watershed occurred at the end of the Visigoth Period and the early Moorish Period (ca 500–700 AD), at around ca 1000 AD, 1450-1500 AD, 1550-1650 AD and since 1700 AD till recent times.

The record provides a coherent paleohydrological reconstruction for the past 1600 years showing an arid period prior to ca 300 AD when the sinkhole was dry, followed by a humid stage at the end of the Roman Period (350AD) when the doline was flooded. The lake has not dried out during the last 1600 years, but experienced large lake level fluctuations: moderate but fluctuating lake levels occurred during the 400-1200 AD period with particularly lower lake levels during 750-850 AD. The highest lake levels occurred during the 1200–1600 AD period. Lake levels decreased after 1600 AD but remained relatively high. Lake level fluctuations frequency was higher during the LIA compared to the MCA.

Although similar paleohydrological evolution occurred in most Iberian lacustrine records, La Parra supports latitudinal gradients within the Iberian Peninsula, with increased humidity during Iberian-Roman times restricted to southern Spain, and early onset of the MCA, and the humid phases of the LIA starting and ending earlier in the central Iberian Range compared to the Pyrenean Domain and southern Spain. Lake La Parra record agrees with a complex pattern of wetter and drier intervals during the LIA. The La Parra record also supports the hypothesis of antiphasic behaviour between Western and Eastern Mediterranean, suggesting an active role for NAO dynamics over the past two millennia in the Western Mediterranean climate patterns. The documented heterogeneity through space and time of

main global climatic phases stresses the need to integrate regional differences in global synthesis.

Acknowledgements

This research has been supported by the GLOBALKARST (CGL2009-08415) and GRACCIE – Consolider CSD2007-00067 projects funded by the Spanish Ministry of Economy and Competitiveness and by the I-LINK program (I-LINK0510) funded by the CSIC. F. Barreiro-Lostres acknowledges the funding from the CSIC "JAE-PreDoc" program. We thank Mark Abbott and the University of Pittsburgh lab staff for their help with the ICP analyses. We also thank Simón Guadalajara, the Regional Government (Junta de Comunidades de Castilla–La Mancha), and numerous colleagues involved in the field campaigns and the IPE-CSIC laboratory services. Authors also want to thank Dr. Penélope González-Sampériz for the help with botanical matters. We also like to thank the two reviewers whose comments and criticisms have helped us to improve the manuscript.

References

Ahmed M, Anchukaitis KJ, Asrat A, Borgaonkar HP, Braida M, Buckley BM, et al. (2013) Continental-scale temperature variability during the past two millennia. *Nature Geoscience* 6(5): 339–346: doi:10.1038/ngeo1797.

Alonso F (1986) Karst Externo. Las torcas de Cuenca. In: Martínez de Pisón E and Tello B (eds) *Atlas de Geomorfología*. Madrid: Alianza, 273–284.

Appleby PG (2001) Chronostratigraphic techniques in recent sediments. In: Last WM and Smol JP (eds) *Tracking Environmental Change Using Lake Sediments, Volume 1: Basin Analysis, Coring, and Chronological Techniques*. Dordrecht: Kluwer Academic Publishers, 171–203.

Barreiro-Lostres F (2012) Depositional evolution of La Parra karstic lake (Iberian Chain, Spain) during the last 1,600 years: Climate and human impact implications. Trabajo fin de máster, Máster de Iniciación a la Investigación en Geología, Zaragoza, España, Universidad de Zaragoza.

Battarbee RW (1986) Diatom analysis. In: Berglund BE (ed) *Handbook of Holocene palaeoecology and palaeohydrology*. Chichester: John Wiley & Sons, 527–570.

Benito G, Díez-Herrero A and Fernández de Villalta M (2003) Magnitude and frequency of flooding in the tagus basin (central spain) over the last millennium. *Climatic Change* 58: 171–192: doi:10.1023/A:1023417102053.

Blaauw M (2010) Methods and code for "classical" age-modelling of radiocarbon sequences. *Quaternary Geochronology* 5(5): 512–518: doi:10.1016/j.quageo.2010.01.002.

Bradley RS (2003) Climate change: Climate in Medieval Time. *Science* 302(5644): 404–405: doi:10.1126/science.1090372.

Bradley RS and Jones PD (1993) "Little Ice Age" summer temperature variations: their nature and relevance to recent global warming trends. *The Holocene* 3(4): 367–376: doi:10.1177/095968369300300409.

Bradley RS (2003) Climate change: Climate in Medieval Time. *Science* 302(5644): 404–405: doi:10.1126/science.1090372.

Brauer A (2004) Annually laminated lake sediments and their palaeoclimatic relevance. In: Fischer H, Kumke T, Lohmann G, Floser G, Miller H, Von Storch V, et al. (eds) *The climate in historical times. Towards a synthesis of Holocene proxy data and climate models*. GKSS, School of Environmental Research. Springer, 109–128.

Burjachs F (1996) La secuencia palinologica de La Cruz (Cuenca, España). In: Ruíz Zapata B, Martín Arroyo T, Valdeolmillos Rodríguez A et al. (eds) *Estudios Palinológicos*. Alcalá: Universidad de Alcalá, pp. 31–36.

Carmona JM and Bitzer K (2001) Los sistemas cársticos de Lagunas de Cañada del Hoyo y Torcas de los Palancares (Serranía de Cuenca. españa). *Las caras del agua subterránea*. Madrid: IGME, 451–460.

Chung FH (1974a) Quantitative interpretation of X-ray diffraction patterns of mixtures. II. Adiabatic principle of X-ray diffraction analysis of mixtures. *Journal of Applied Crystallography* 7(6): 526–531: doi:10.1107/S0021889874010387.

Chung FH (1974b) Quantitative interpretation of X-ray diffraction patterns of mixtures. I. Matrix-flushing method for quantitative multicomponent analysis. *Journal of Applied Crystallography* 7(6): 519–525: doi:10.1107/S0021889874010375.

Corella JP, Amrani AE, Sigró J, Morellón M, Rico E and Valero-Garcés BL (2011) Recent evolution of Lake Arreo, northern Spain: influences of land use change and climate. *Journal of Paleolimnology* 46(3): 469–485: doi:10.1007/s10933-010-9492-7.

Corella JP, Moreno A, Morellón M, Rull V, Giralt S, Rico MT, et al. (2010) Climate and human impact on a meromictic lake during the last 6,000 years (Montcortès Lake, Central Pyrenees, Spain). *Journal of Paleolimnology* 46(3): 351–367: doi:10.1007/s10933-010-9443-3.

Corella JP, Amrani AE, Sigró J, Morellón M, Rico E and Valero-Garcés BL (2011) Recent evolution of Lake Arreo, northern Spain: influences of land use change and climate. *Journal of Paleolimnology* 46(3): 469–485: doi:10.1007/s10933-010-9492-7.

Corella JP, Brauer A, Mangili C, Rull V, Vegas-Vilarrúbia T, Morellón M, et al. (2012) The 1.5-ka varved record of Lake Montcortès (southern Pyrenees, NE Spain). *Quaternary Research* 78(2): 323–332: doi:10.1016/j.yqres.2012.06.002.

Corella JP, Moreno A, Morellón M, Rull V, Giralt S, Rico MT, et al. (2010) Climate and human impact on a meromictic lake during the last 6,000 years (Montcortès Lake, Central Pyrenees, Spain). *Journal of Paleolimnology* 46(3): 351–367: doi:10.1007/s10933-010-9443-3.

Corella JP, Stefanova V, El Anjoumi A, Rico E, Giralt

S, Moreno A, et al. (2013) A 2500-year multi-proxy reconstruction of climate change and human activities in northern Spain: The Lake Arreo record. *Palaeogeography, Palaeoclimatology, Palaeoecology* 386: 555–568: doi:10.1016/j.palaeo.2013.06.022.

Creus Novau J (2000) Dendrocronología y dendroclimatología, o cómo los árboles nos cuentan el clima del pasado. In: García Cordón JC (ed) *La reconstrucción del clima de época preinstrumental*. Santander: Universidad de Cantabria, 81–122.

Currás A, Zamora L, Reed JM, García-Soto E, Ferrero S, Armengol X, et al. (2012) Climate change and human impact in central Spain during Roman times: High-resolution multi-proxy analysis of a tufa lake record (Somolinos, 1280m asl). *Catena* 89(1): 31–53: doi:10.1016/j.catena.2011.09.009.

Díaz HF, Trigo R, Hughes MK, Mann ME, Xoplaki E and Barriopedro D (2011) Spatial and Temporal Characteristics of Climate in Medieval Times Revisited. *Bulletin of the American Meteorological Society* 92(11): 1487–1500. doi:10.1175/BAMS-D-10-05003.1.

Domínguez-Castro F, Santisteban JI, Barriendos M and Mediavilla R (2008) Reconstruction of drought episodes for central Spain from rogation ceremonies recorded at the Toledo Cathedral from 1506 to 1900: A methodological approach. *Global and Planetary Change* 63(2-3): 230–242. doi:10.1016/j.gloplacha.2008.06.002.

Domínguez-Castro F, de Miguel JC, Vaquero JM, Gallego MC and Garcia-Herrera R (2014) Climatic potential of Islamic chronicles in Iberia: Extreme droughts (AD 711-1010). *The Holocene* 24: 370–374. doi:10.1177/0959683613518591.

Eraso A, López-Acevedo V, López M, Navarro V, Suso J and Santos V (1979) *Estudio De Las Torcas De Palancares Y Cañada Del Hoyo En El Karst De La Serranía De Cuenca*. Bilbao: Kobie.

Fletcher WJ and Zielhofer C (2013) Fragility of Western Mediterranean landscapes during Holocene Rapid Climate Changes. *CATENA* 103: 16–29: doi:10.1016/j.catena.2011.05.001.

Gil-Romera G, Carrión JS, Pausas JG, Sevilla-Callejo M, Lamb HF, Fernández S, et al. (2010) Holocene fire activity and vegetation response in South-Eastern Iberia. *Quaternary Science Reviews* 29(9-10): 1082–1092: doi:10.1016/j.quascirev.2010.01.006. 259(2-3): 157–181: doi:10.1016/j.palaeo.2007.10.005.

Gutiérrez Elorza M and Valverde M (1994) El sistema de poljes del río Guadazaón (Cordillera Ibérica, prov. de Cuenca). *Cuaternario y Geomorfología* 8(1-2): 87–95.

Gutiérrez-Elorza M and Peña-Monné JL (1998) Geomorphology and late Holocene climatic change in Northeastern Spain. *Geomorphology* 23(2): 205–217.

Gutiérrez F, Calaforra JM, Cardona F, Ortí F, Durán JJ and Garay P (2008) Geological and environmental implications of the evaporite karst in Spain. *Environmental Geology* 53(5): 951–965: doi:10.1007/s00254-007-0721-y.

Håkansson H and Carter JR (1990) An Interpretation of HUSTEDT's Terms" Schattenlinie"" Perlenreihe" and" Höcker" Using Specimens of the Cyclotella radiosacomplex, C. distinguenda HUST. and C. cyclopuncta nov. spec. *Jour. Iowa Acad. Sci* (97): 153–156.

Håkansson H (2002) A compilation and evaluation of species in the genera Stephanodiscus, Cycclostephanos and Cyclotella with a new genus in the family Stephanodiscaceae. *Diatom Research* 17: 1–139.

Höbig N, Weber ME, Kehl M, Weniger G-C, Julià R, Melles M, et al. (2012) Lake Banyoles (northeastern Spain): A Last Glacial to Holocene multi-proxy study with regard to environmental variability and human occupation. *Quaternary International* 274: 205–218: doi:10.1016/j.quaint.2012.05.036.

Hughes MK and Diaz HF (1994) Was there a "Medieval Warm Period", and if so, where and when? *Climatic Change* 26(2-3): 109–142.

IGME (1973) *Mapa Geológico de España. 1:50.000.* (Serie Magna). Hoja 635. Fuentes. Madrid: Servicio de Publicaciones, Ministerio de Industria y Energía, 1 map.

IGN (2002) *Mapa Topográfico Nacional. 1:25.000.* Hoja de Fuentes, 635-II. Servicio de Publicaciones, Ministerio de Fomento, 1 map.

Jones MD, Roberts CN, Leng MJ and Türkeş M (2006) A high-resolution late Holocene lake isotope record from Turkey and links to North Atlantic and monsoon climate. *Geology* 34(5): 361: doi:10.1130/G22407.1.

Jones PD, Briffa KR, Osborn TJ, Lough JM, van Ommen TD, Vinther BM, et al. (2009) High-resolution palaeoclimatology of the last millennium: a review of current status and future prospects. *The Holocene* 19(1): 3–49: doi:10.1177/0959683608098952.

Julià R, Burjachs F, Dasi M, Mezquita F, Miracle M, Roca J, et al. (1998) Meromixis origin and recent trophic evolution in the Spanish mountain lake La Cruz. *Aquatic Sciences* 60(4): 279–299.

Kiss KT, Ács É, Szabó KÉ, Miracle MR and Vicente E (2007) Morphological Observations on Cyclotella Distinguenda Hustedt and C. Delicatula Hustedt from the Core Sample of a Meromictic Karstic Lake of Spain (lake La Cruz) with Aspects of Their Ecology. *Diatom Research* 22(2): 287–308: doi:10.1080/0269249X.2007.9705716.

Köster D and Pienitz R (2006) Seasonal Diatom Variability and Paleolimnological Inferences – A Case Study. *Journal of Paleolimnology* 35(2): 395–416: doi:10.1007/s10933-005-1334-7.

Krammer K and Lange-Bertalot H (1986-1991) *Süswasser flora von Mitteleuropa* 2 (Teil 1-4). Stuttgart-Jena, Germany: VEB Gustav Fischer, Germany.

Lamb HH (1965) The early medieval warm epoch

and its sequel. *Palaeogeography, Palaeoclimatology, Palaeoecology* 1: 13–37.

Lebreiro SM, Francés G, Abrantes FFG, Diz P, Bartels-Jónsdóttir HB, Stroynowski ZN, et al. (2006) Climate change and coastal hydrographic response along the Atlantic Iberian margin (Tagus Prodelta and Muros Ría) during the last two millennia. *The Holocene* 16(7): 1003–1015: doi:10.1177/0959683606hl990rp.

Leira M (2005) Diatom responses to Holocene environmental changes in a small lake in northwest Spain. *Quaternary International* 140–141: 90–102: doi:10.1016/j.quaint.2005.05.005.

Lionello P (ed) (2012) *The climate of the Mediterranean region: from the past to the future*. London ; Waltham, MA: Elsevier.

López-Blanco C, Gaillard M-J, Miracle MR and Vicente E (2011) Lake-level changes and fire history at Lagunillo del Tejo (Spain) during the last millennium: Climate or humans? *The Holocene* 22(5): 551–560: doi:10.1177/0959683611427337.

López-Merino L, Moreno A, Leira M, Sigró J, González-Sampériz P, Valero-Garcés BL, et al. (2011) Two hundred years of environmental change in Picos de Europa National Park inferred from sediments of Lago Enol, northern Iberia. *Journal of Paleolimnology* 46(3): 453–467: doi:10.1007/s10933-011-9546-5.

López-Sáez JA, Abel-Schaad D, Pérez-Díaz S, Blanco-González A, Alba-Sánchez F, Dorado M, et al. (in press) Vegetation history, climate and human impact in the Spanish Central System over the last 9000 years. *Quaternary International*. doi:10.1016/j.quaint.2013.06.034.

Lozano-Sahuquillo V (2002) *La Cañada del Hoyo de Cuenca: su Personalidad Histórica*. Cartagena: LOYGA.

Luque J. and Julià R (2002) Lake sediment response to land-use and climate change during the last 1000 years in the oligotrophic Lake Sanabria (northwest of Iberian Peninsula). *Sedimentary Geology* 148(1–2): 343–355: doi:10.1016/S0037-0738(01)00225-1.

Magny M, Peyron O, Sadori L, Ortu E, Zanchetta G, Vannière B, et al. (2012) Contrasting patterns of precipitation seasonality during the Holocene in the south- and north-central Mediterranean. *Journal of Quaternary Science* 27(3): 290–296: doi:10.1002/jqs.1543.

Magny M, Combourieu Nebout N, de Beaulieu JL, Bout-Roumazeilles V, Colombaroli D, Desprat S, et al. (2013) North–south palaeohydrological contrasts in the central Mediterranean during the Holocene: tentative synthesis and working hypotheses. *Climate of the Past Discussions* 9(2): 1901–1967: doi:10.5194/cpd-9-1901-2013.

Magny M, Peyron O, Sadori L, Ortu E, Zanchetta G, Vannière B, et al. (2012) Contrasting patterns of precipitation seasonality during the Holocene in the south- and north-central Mediterranean. *Journal of Quaternary Science* 27(3): 290–296: doi:10.1002/jqs.1543.

Mann ME, Zhang Z, Rutherford S, Bradley RS, Hughes MK, Shindell D, et al. (2009) Global Signatures and Dynamical Origins of the Little Ice Age and Medieval Climate Anomaly. *Science* 326 (5957): 1256–1260: doi:10.1126/science.1177303.

Martínez-Cortizas A, Pontevedra-Pombal X, García-Rodeja E, Nóvoa-Muñoz JC and Shotyk W (1999) Mercury in a Spanish Peat Bog: Archive of Climate Change and Atmospheric Metal Deposition. *Science* 284(5416): 939–942: doi:10.1126/science.284.5416.939.

Martín-Puertas C, Valero-Garces BL, Pilar Mata M, Gonzalez-Samperiz P, Bao R, Moreno A, et al. (2008) Arid and humid phases in southern Spain during the last 4000 years: the Zonar Lake record, Cordoba. *The Holocene* 18(6): 907–921: doi:10.1177/0959683608093533.

Martín-Puertas C, Valero-Garcés BL, Mata MP, Moreno A, Giralt S, Martínez-Ruiz F, et al. (2009) Geochemical processes in a Mediterranean Lake: a high-resolution study of the last 4,000 years in Zoñar Lake, southern Spain. *Journal of Paleolimnology* 46(3): 405–421: doi:10.1007/s10933-009-9373-0.

Martín-Puertas C, Valero-Garces BL, Pilar Mata M, Gonzalez-Samperiz P, Bao R, Moreno A, et al. (2008) Arid and humid phases in southern Spain during the last 4000 years: the Zonar Lake record, Cordoba. *The Holocene* 18(6): 907–921: doi:10.1177/0959683608093533.

Mayewski P, Rohling E, Curtstager J, Karlen W, Maasch K, Davidmeeker L, et al. (2004) Holocene climate variability. *Quaternary Research* 62(3): 243–255: doi:10.1016/j.yqres.2004.07.001.

Meyers P and Lallier-vergés E (1999) Lacustrine Sedimentary Organic Matter Records of Late Quaternary Paleoclimates. *Journal of Paleolimnology* 21(3): 345–372.

Miracle MR, Vicente E and Pedrós-Alió C (1992) Biological studies of Spanish meromictic and stratified karstic lakes. *Limnetica* 8: 59–77.

Morellón M, Valero-Garcés B, Moreno A, González-Sampériz P, Mata P, Romero O, et al. (2008) Holocene palaeohydrology and climate variability in northeastern Spain: The sedimentary record of Lake Estanya (Pre-Pyrenean range). *Quaternary International* 181(1): 15–31.

Morellón M, Valero-Garcés B, González-Sampériz P, Vegas-Vilarrúbia T, Rubio E, Rieradevall M, et al. (2011) Climate changes and human activities recorded in the sediments of Lake Estanya (NE Spain) during the Medieval Warm Period and Little Ice Age. *Journal of Paleolimnology* 46(3): 423–452: doi:10.1007/s10933-009-9346-3.

Morellón M, Valero-Garcés B, Moreno A, González-Sampériz P, Mata P, Romero O, et al. (2008) Holocene palaeohydrology and climate variability in northeastern Spain: The sedimentary record of Lake Estanya (Pre-Pyrenean range). *Quaternary International* 181(1): 15–31.

Moreno A, Valero-Garcés BL, González-Sampériz P and Rico M (2008) Flood response to rainfall variability during the last 2000 years inferred from the Taravilla Lake record (Central Iberian Range, Spain). *Journal of Paleolimnology* 40(3): 943–961: doi:10.1007/s10933-008-9209-3.

Moreno A, López-Merino L, Leira M, Marco-Barba J, González-Sampériz P, Valero-Garcés BL, et al. (2009) Revealing the last 13,500 years of environmental history from the multiproxy record of a mountain lake (Lago Enol, northern Iberian Peninsula). *Journal of Paleolimnology* 46(3): 327–349: doi:10.1007/s10933-009-9387-7.

Moreno A, Pérez A, Frigola J, Nieto-Moreno V, Rodrigo-Gámiz M, Martrat B, et al. (2012) The Medieval Climate Anomaly in the Iberian Peninsula reconstructed from marine and lake records. *Quaternary Science Reviews* 43: 16–32: doi:10.1016/j.quascirev.2012.04.007.

Neumann FH, Kagan EJ, Schwab MJ et al. (2007) Palynology, sedimentology and palaeoecology of the late Holocene Dead Sea. *Quaternary Science Reviews* 26: 1476–1498.

Nieto-Moreno V, Martínez-Ruiz F, Giralt S, Jiménez-Espejo F, Gallego-Torres D, Rodrigo-Gámiz M, et al. (2011) Tracking climate variability in the western Mediterranean during the Late Holocene: a multiproxy approach. *Clim. Past* 7(4): 1395–1414: doi:10.5194/cp-7-1395-2011.

Nieto-Moreno V, Martínez-Ruiz F, Giralt S, Jiménez-Espejo F, Gallego-Torres D, Rodrigo-Gámiz M, et al. (2011) Tracking climate variability in the western Mediterranean during the Late Holocene: a multiproxy approach. *Clim. Past* 7(4): 1395–1414: doi:10.5194/cp-7-1395-2011.

Nieto-Moreno V, Martinez-Ruiz F, Giralt S, Gallego-Torres D, Garcia-Orellana J, Masque P, et al. (2013) Climate imprints during the "Medieval Climate Anomaly" and the "Little Ice Age" in marine records from the Alboran Sea basin. *The Holocene* 23(29): 1227–1237: doi:10.1177/0959683613484613.

Oksanen J, Blanchet FG, Kindt R, Legendre P, Minchin PR, O'Hara RB, et al. (2013) vegan: Community Ecology Package. R package version 2.0-10.

Pèlachs A, Pérez-Obiol R, Ninyerola M and Nadal J (2009) Landscape dynamics of Abies and Fagus in the southern Pyrenees during the last 2200 years as a result of anthropogenic impacts. *Review of Palaeobotany and Palynology* 156(3-4): 337–349: doi:10.1016/j.revpalbo.2009.04.005.

Pérez-Lambán F, Peña-Monné JL, Fanlo-Loras J, Picazo-Millán JV, Badia-Villas D, Rubio-Fernández V, et al. (2013) Paleoenvironmental and geoarchaeological reconstruction from late Holocene slope records (Lower Huerva Valley, Ebro Basin, NE Spain). *Quaternary Research*. doi:10.1016/j.yqres.2013.10.011.

Pla S and Catalán J (2005) Chrysophyte cysts from lake sediments reveal the submillennial winter/spring climate variability in the northwestern Mediterranean region throughout the Holocene. *Climate Dynamics* 24(2-3): 263–278: doi:10.1007/s00382-004-0482-1.

Pompeani DP, Abbott MB, Steinman BA and Bain DJ (2013) Lake Sediments Record Prehistoric Lead Pollution Related to Early Copper Production in North America. *Environmental Science & Technology* 47(11): 5545–5552: doi:10.1021/es304499c.

R Development Core Team (2013) *R: A language and environment for statistical computing*. R Foundation for Statistical Computing Vienna, Austria.

Reed JM (1998) Diatom preservation in the recent sediment record of Spanish saline lakes: implications for palaeoclimate study. *Journal of Paleolimnology* 19(2): 129–137.

Reed JM, Stevenson AC and Juggins S (2001) A multi-proxy record of Holocene climatic change in southwestern Spain: the Laguna de Medina, Cádiz. *The Holocene* 11(6): 707–719: doi:10.1191/09596830195735.

Reimer PJ, Baillie MGL, Bard E, Bayliss A, Beck JW, Blackwell PG, et al. (2009) INTCAL 09 and MARINE09 aadiocarbon age calibration curves, 0-50,000 years Cal BP. *Radiocarbon* 51(4): 1111–1150.

Riera S, Wansard G and Julià R (2004) 2000-year environmental history of a karstic lake in the Mediterranean Pre-Pyrenees: the Estanya lakes (Spain). *CATENA* 55(3): 293–324: doi:10.1016/S0341-8162(03)00107-3.

Roberts N, Brayshaw D, Kuzucuoglu C, Perez R and Sadori L (2011) The mid-Holocene climatic transition in the Mediterranean: Causes and consequences. *The Holocene* 21(1): 3–13: doi:10.1177/0959683610388058.

Roberts N, Moreno A, Valero-Garcés BL, Corella JP, Jones M, Allcock S, et al. (2012) Palaeolimnological evidence for an east–west climate see-saw in the Mediterranean since AD 900. *Global and Planetary Change* 84-85: 23–34: doi:10.1016/j.gloplacha.2011.11.002.

Rodrigo FS and Barriendos M (2008) Reconstruction of seasonal and annual rainfall variability in the Iberian peninsula (16th–20th centuries) from documentary data. *Global and Planetary Change* 63(2-3): 243–257: doi:10.1016/j.gloplacha.2007.09.004.

Rodrigo M, Miracle M and Vicente E (2001) The meromictic Lake La Cruz (Central Spain). Patterns of stratification. *Aquatic Sciences* 63(4): 406–416.

Romero-Viana L, Julià R, Camacho A, Vicente E and Miracle MR (2008) Climate Signal in Varve Thickness: Lake La Cruz (spain), a Case Study. *Journal of Paleolimnology* 40(2): 703–714: doi:10.1007/s10933-008-9194-6.

Romero-Viana L, Keely BJ, Camacho A, Vicente E and Miracle MR (2009a) Primary production in Lake La Cruz (Spain) over the last four centuries: reconstruction based on sedimentary signal of

photosynthetic pigments. *Journal of Paleolimnology* 43(4): 771–786: doi:10.1007/s10933-009-9367-y.

Romero-Viana L, Miracle MR, López-Blanco C, Cuna E, Vilaclara G, Garcia-Orellana J, et al. (2009b) Sedimentary multiproxy response to hydroclimatic variability in Lagunillo del Tejo (Spain). *Hydrobiologia* 631(1): 231–245: doi:10.1007/s10750-009-9813-x.

Romero-Viana L, Julià R, Schimmel M, Camacho A, Vicente E and Miracle MR (2011) Reconstruction of annual winter rainfall since A.D.1579 in central-eastern Spain based on calcite laminated sediment from Lake La Cruz. *Climatic Change* 107(3-4): 343–361: doi:10.1007/s10584-010-9966-7.

JC and Valle-Melendo J del (2005) Estudio de la evolución de régimen hidrológico en zonas húmedas drenadas: los humedales del Cañizar (Provincia de Teruel, España). *Investigaciones geográficas, 38, 2005; pp. 47-63.*

Saz-Sánchez MA (2003) *Temperaturas y precipitaciones en la mitad norte de España desde el siglo XV. Estudio dendroclimático*. Zaragoza: Consejo de Protección de la Naturaleza de Aragón.

Scussolini P, Vegas-Vilarrúbia T, Rull V, Corella JP, Valero-Garcés B and Gomà J (2011) Middle and late Holocene climate change and human impact inferred from diatoms, algae and aquatic macrophyte pollen in sediments from Lake Montcortès (NE Iberian Peninsula). *Journal of Paleolimnology* 46(3): 369–385: doi:10.1007/s10933-011-9524-y.

Schnurrenberger D, Russell J and Kelts K (2003) Classification of lacustrine sediments based on sedimentary components. *Journal of Paleolimnology* 29(2): 141–154.

Simonneau A, Chapron E, Courp T, Tachikawa K, Le Roux G, Baron S, et al. (2013) Recent climatic and anthropogenic imprints on lacustrine systems in the Pyrenean Mountains inferred from minerogenic and organic clastic supply (Vicdessos valley, Pyrenees, France). *The Holocene* 23(12): 1764–1777: doi:10.1177/0959683613505340.

Stoermer EF, Emmert G, Julius ML and Schelske CL (1996) Paleolimnologic evidence of rapid recent change in Lake Erie's trophic status. *Canadian Journal of Fisheries and Aquatic Sciences* 53(6): 1451–1458: doi:10.1139/f96-067.

Trouet V, Esper J, Graham NE, Baker A, Scourse JD and Frank DC (2009) Persistent Positive North Atlantic Oscillation Mode Dominated the Medieval Climate Anomaly. *Science* 324(5923): 78–80: doi:10.1126/science.1166349.

Valero-Garcés BL and Moreno A (2011) Iberian lacustrine sediment records: responses to past and recent global changes in the Mediterranean region. *Journal of Paleolimnology* 46(3): 319–325: doi:10.1007/s10933-011-9559-0.

Valero-Garcés B, Morellón M, Moreno A, Corella JP, Martín-Puertas C, Barreiro F, et al. (2014) Lacustrine carbonates of Iberian Karst Lakes: Sources, processes and depositional environments. *Sedimentary Geology* 299: 1–29: doi:10.1016/j.sedgeo.2013.10.007.

Wanner H, Beer J, Butikofer J, Crowley T, Cubasch U, Fluckiger J, et al. (2008) Mid- to Late Holocene climate change: an overview. *Quaternary Science Reviews* 27(19-20): 1791–1828: doi:10.1016/j.quascirev.2008.06.013.

Wirth SB, Gilli A, Simonneau A, Ariztegui D, Vannière B, Glur L, et al. (2013) A 2000 year long seasonal record of floods in the southern European Alps. *Geophysical Research Letters* 40(15): 4025–4029: doi:10.1002/grl.50741.

Xoplaki E, González-Rouco JF, Luterbacher J and Wanner H (2004) Wet season Mediterranean precipitation variability: influence of large-scale dynamics and trends. *Climate Dynamics* 23(1): 63–78: doi:10.1007/s00382-004-0422-0.

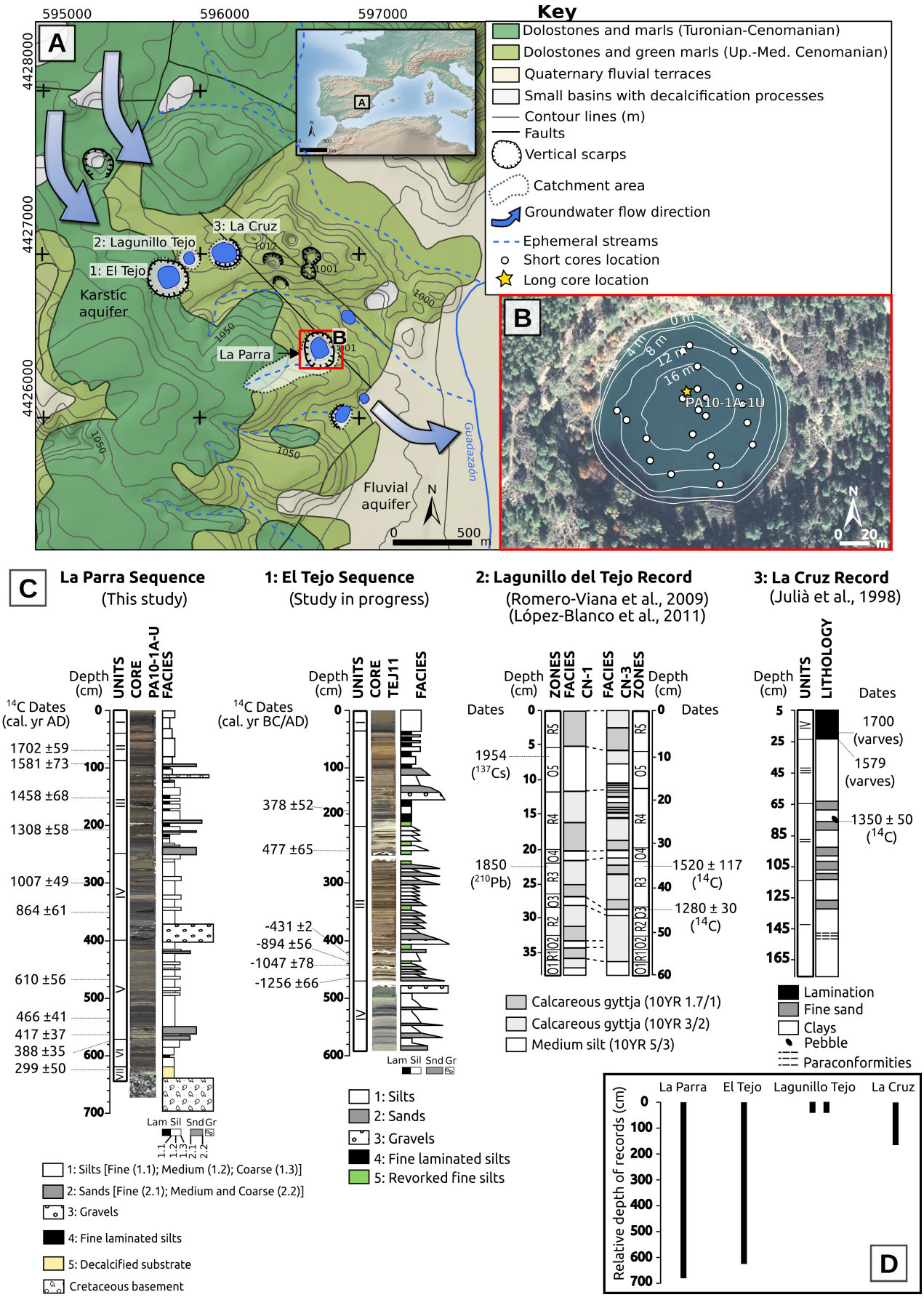

Figure 1. A) Location of study site and detailed geological map of the lake complex from Cañada del Hoyo (based on IGME, (1973) and IGN (2002). B) Lake La Parra bathymetry with short cores (white dots) and long core PA10-1A-U (yellow star) location. C: Cores recovered up to date on the lake complex in depth with the main dates and sediment stratigraphy (1: El Tejo; 2: El Lagunillo del Tejo; 3: La Cruz). D: Relative depth of each record.

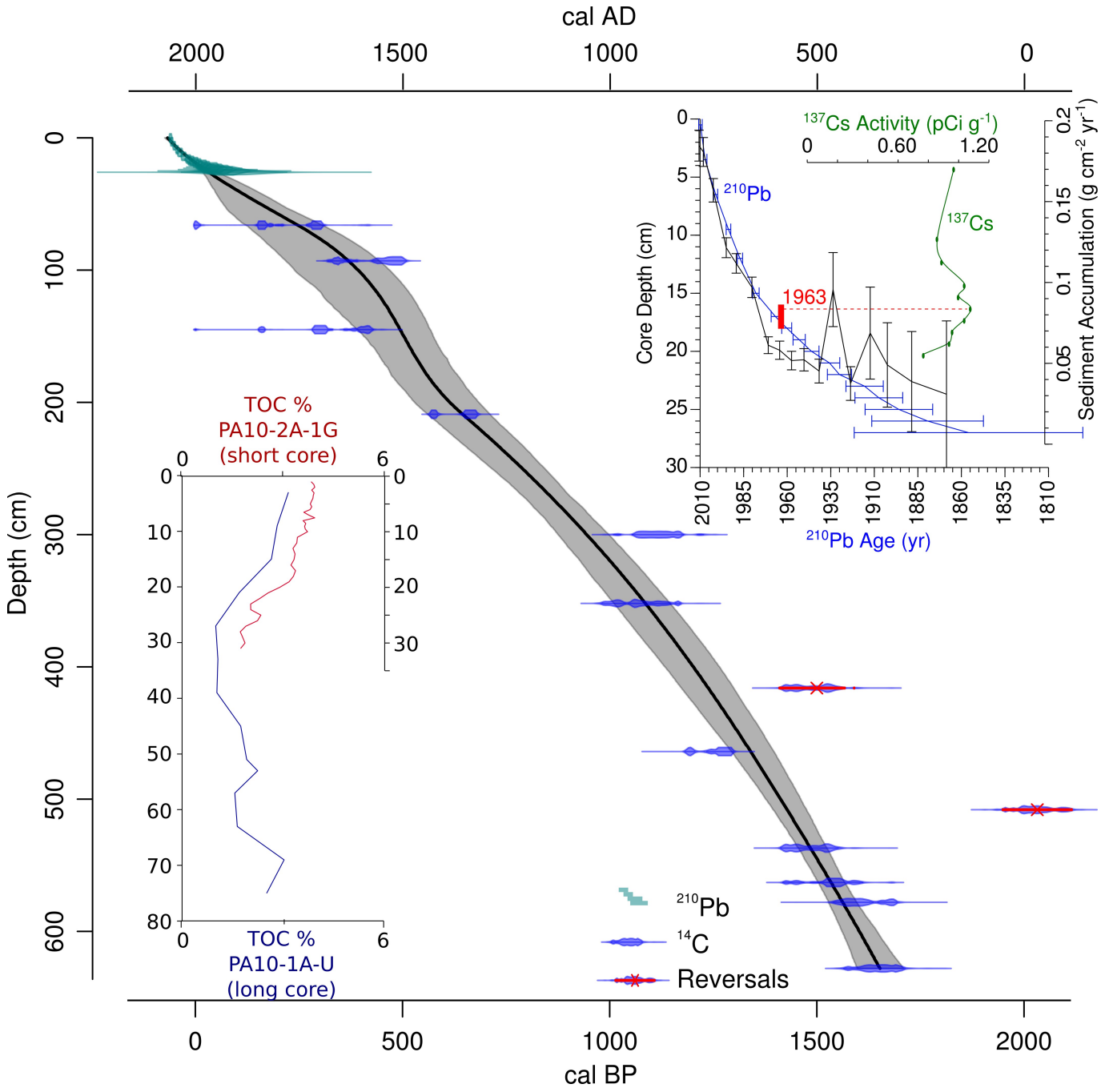

Figure 2. Chronological model of the studied sequence based on weighted spline regression (Blaauw, 2010) of 13 AMS ^{14}C dates from the long core (blue lines) and ^{210}Pb dates (green lines) from the short core. Two reversal dates are also represented (red crossed dates). The black continuous line represents the age-depth function framed by error lines (grey shaded area). At top-right is showed the agreement between ^{137}Cs and ^{210}Pb dating, and the sediment accumulation rate for the first 30 cm of the core. At bottom-left is represented the good correlation between the short core PA10-21-1G (red) and the main long core PA10-1A-U (blue) using TOC (%) values.

Table 1. Radiocarbon dates used for the construction of the age model for the Lake La Parra sequence. Dates were calibrated using CLAM software (Blaauw, 2010) and the INTCAL09 curve (Reimer et al., 2009); and the 2σ probability interval was selected. Dates with * were discarded (reversals or stratigraphically inconsistent).

Core depth (cm)	Laboratoy code	^{14}C AMS age (BP)	2σ calibrated age (cal. yr. AD)	Material
66	Poz-37954	230 ± 30	1660 ± 24	Wood fragment
93	Poz-37955	390 ± 35	1482 ± 42	Wood fragment
145	Poz-37956	265 ± 30	1644 ± 26	Wood fragment
209	D-AMS 1217-210	693 ± 25	1296 ± 28	Wood fragment
300	Poz-37957	1190 ± 30	834 ± 64	Wood fragment
352	Poz-37958	1155 ± 30	854 ± 53	Wood fragment
416	D-AMS 1217-211	1614 ± 34	462 ± 80*	Wood fragment
464	D-AMS 1217-212	1328 ± 28	684 ± 34	Wood fragment
508	Poz-37959	2060 ± 30	-83 ± 84*	Wood fragment
537	D-AMS 1217-213	1609 ± 30	490 ± 93	Wood fragment
563	Poz-37960	1640 ± 30	403 ± 65	Wood fragment
578	Poz-37962	1700 ± 30	362 ± 49	Wood fragment
628	Poz-37963	1740 ± 30	311 ± 75	Wood fragment

Table 2. La Parra sedimentary facies: description, composition and depositional processes and environments. TIC, TOC, and TOC/TN are averaged values for each facies.

Lithology	*Facies*	*Description*	*Depositional Processes*	*Depositional Environments*
Clastic facies				
Silts	**1.1** ***Fine dark silts***	Dark grey and black, massive carbonate and quartz fine silts, with abundant diatoms and amorphous Organic Matter (OM) in 10-25 cm thick beds with gradational (dark grey). and sharp (black beds) boundaries. TIC: 8% TOC: 3% TOC/TN: 15	Low energy tractive currents and out of suspension	Profundal-distal, deeper areas, alternating oxygenated and anoxic conditions
	1.2 ***Medium brown silts***	Dark and light brown, banded, carbonate and quartz silts, with macrophyte remains in 5-20 cm thick layers with diffuse boundaries. TIC: 7% TOC: 2% TOC/TN: 14	Low energy tractive currents. Frequent redox changes	Profundal-distal to proximal, relatively deep, dominant oxygenated conditions.
	1.3 ***Coarse grey silts***	Light grey and dark massive carbonate and quartz silts with abundant mm-sized, OM fragments and presence of ostracods and some disperse carbonatic cm-long pebbles. They appear in fining-upwards beds, 2-10 cm thick, with irregular basal boundaries. TIC: 8% TOC: 3% TOC/TN: 12	Flood events	Profundal-distal to proximal oxygenated, moderate depth
Sands	**2.1** ***Fine green sands***	Greenish, massive sands dominated by angular carbonate and quartz grains with a greenish silty matrix. They occur in few 3-4 cm thick beds. TIC: 7% TOC: 1% TOC/TN: 11	High energy alluvial tractive currents	Littoral to proximal, shallow, with strong alluvial influence
	2.2 ***Medium and coarse brown sands***	Brown, massive sands dominated by angular carbonate and quartz grains with a fine-medium silty matrix in 2-10 cm thick beds with irregular boundaries. Coarse sands occur in a single 10 cm thick bed with irregular boundaries.. TIC: 9% TOC: 2% TOC/TN: 30		
Gravels	**3** ***Fine and Medium brown gravels***	Brown, massive gravel composed of carbonate, angular clasts (2-25 mm) in a silty matrix. They occur in a single 30 cm thick bed with irregular boundaries. Fine gravels occur in a single 2 cm thick bed, 0.5-2 mm clasts, and present some invertebrate exoskeleton fragments. TIC: 8% TOC: 1% TOC/TN: 9	High energy alluvial tractive currents	Littoral, shallow, with strong alluvial influence
Laminated, endogenic carbonate facies				
Silts	**4** ***Fine laminated silts***	Sets of 5 cm thick intervals composed of 1 mm thick white calcitic and dark OM-rich laminae with net and regular boundaries. Organic layer shows a high amount of diatoms and amorphous organic matter and calcite layer is mostly composed of ~25 µm long homometric subidiomorphous calcite grains. TIC: 9% TOC: 3% TOC/TN: 10	Out of suspension organic deposition, endogenic calcite bioproduction	Profundal-distal, permanently or seasonally anoxic
Substrate				
Breccia	**5** ***Decalcified substrate***	Whitish, massive mixture of angular, irregularly-shaped carbonate fragments (2-30 mm),embedded in a green coarse-silty matrix. TIC: 2% TOC: <1% TOC/TN: <8%	Karstic processes: washing decalcification, dissolution and brecciation of carbonate substrate.	Dry doline

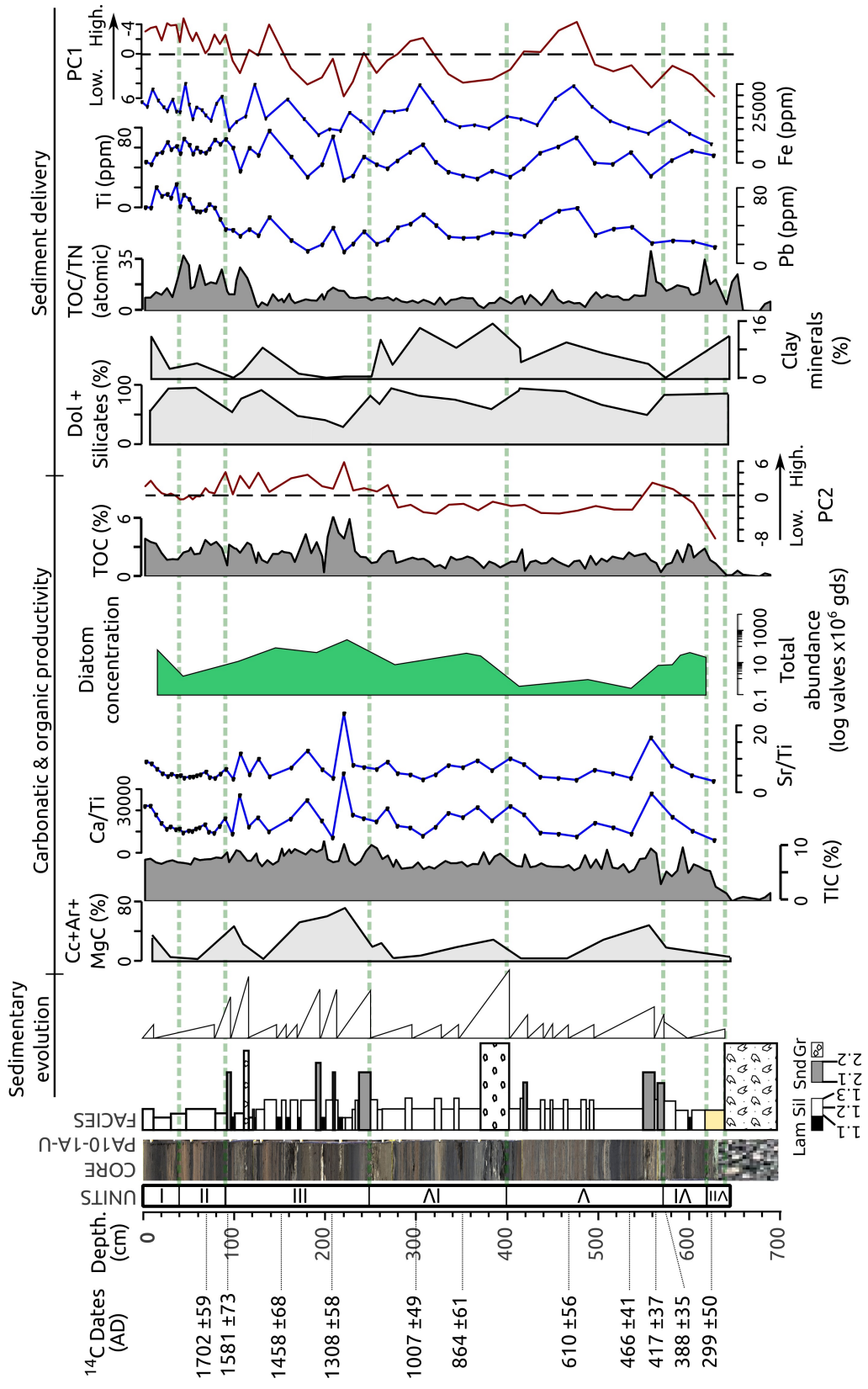

Figure 3. Sedimentary sequence of the PA10-1A-U core in depth (cm), with subdivision in units, core image, sediment stratigraphy and sedimentary evolution organized mostly in fining-upward sequences. Profiles for detrital (Do: Dolomite and Silicates), clays and endogenic (Cc: Calcite, Ar: Aragonite and MgC: Magnesian Calcite) minerals are expressed in percentages. Geochemical stratigraphy shows main quantitative ICP ratios (Ca/Ti, Sr/Ti) and Pb, Ti and Fe values (blue dotted lines), expressed in ppm. First (PC1) and second (PC2) principal components of the Principal Component Analysis (PCA) are plotted in red. Negative values of the first PCA eigenvector (PC1) represent increased detrital input, while positive values of the second eigenvector (PC2) are interpreted as higher biological productivity. TIC (%), TOC (%) and TOC/TN (atomic) values along the sequence are represented in dark gray. Dates are cal. yr AD.

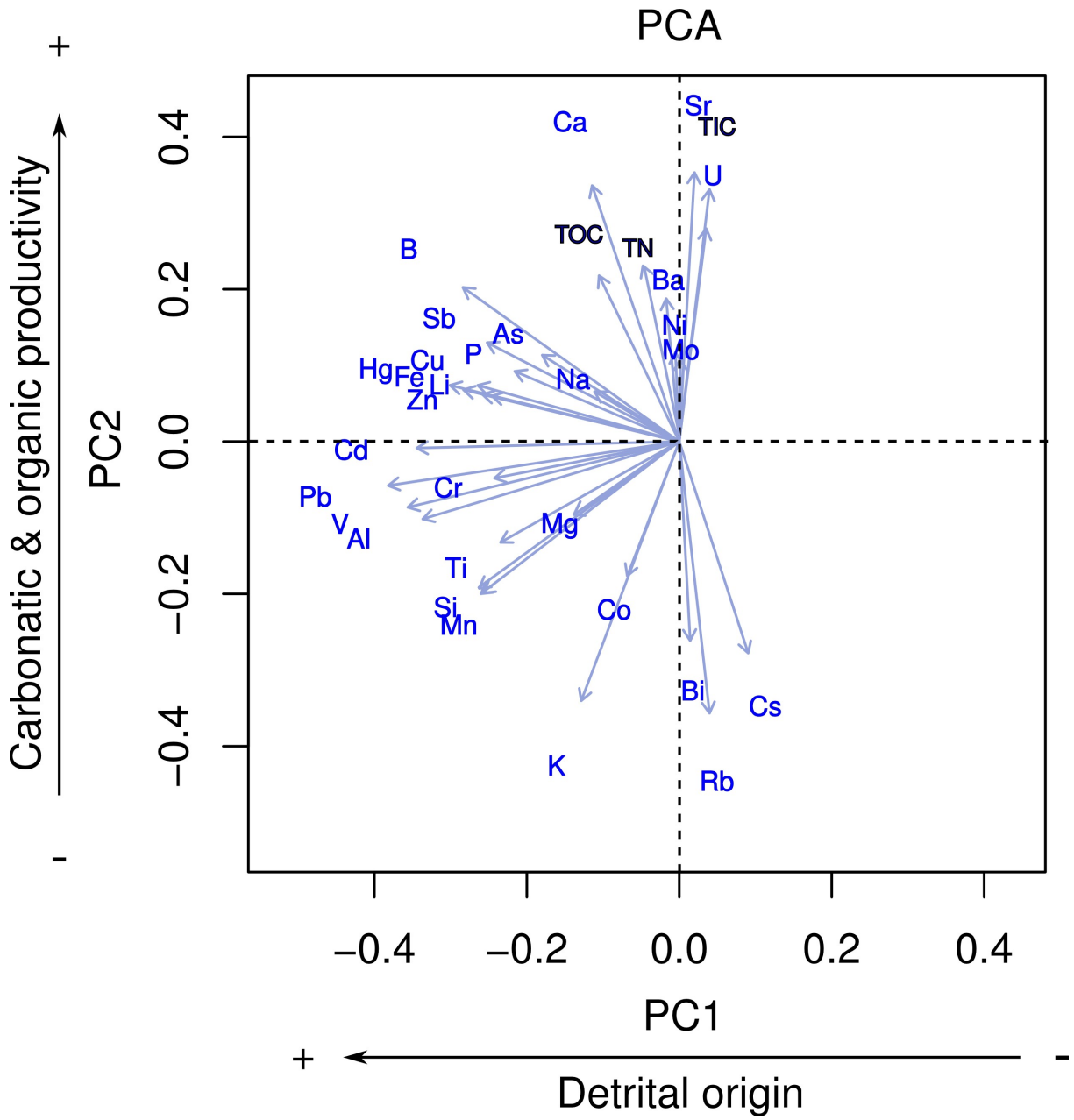

Figure 4. Principal Component Analysis (PCA) of the PA10-1A-1U core geochemical composition (TOC, TIC, TOC/TN -black- and major and trace elements from ICP –blue-). Dataset contains 35 variables and 52 cases. The first eigenvector (PC1) highlights the detrital inputs, whereas the second eigenvector (PC2) has been interpreted as changes in carbonatic and organic productivity.

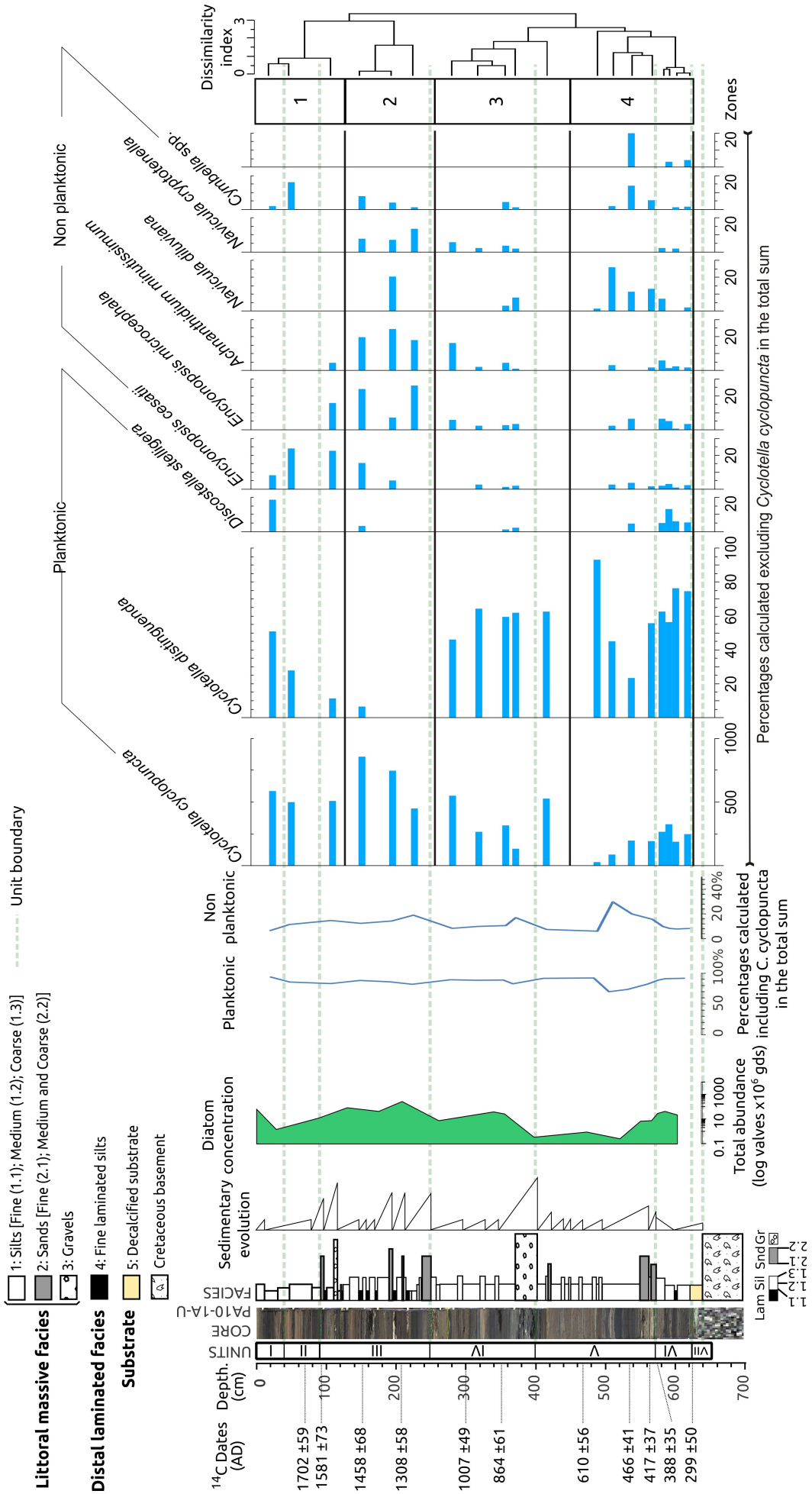

Figure 5. Main diatom species distribution in La Parra sequence. The most abundant species are planktonic *C. cyclopuncta* and *C. distinguenda*; Non-planktonic group includes benthonic and tychoplanktonic species. Values are expressed in percentages, excluding *Cyclotella*. Diatom concentrations are expressed in valves per gram of sediment.

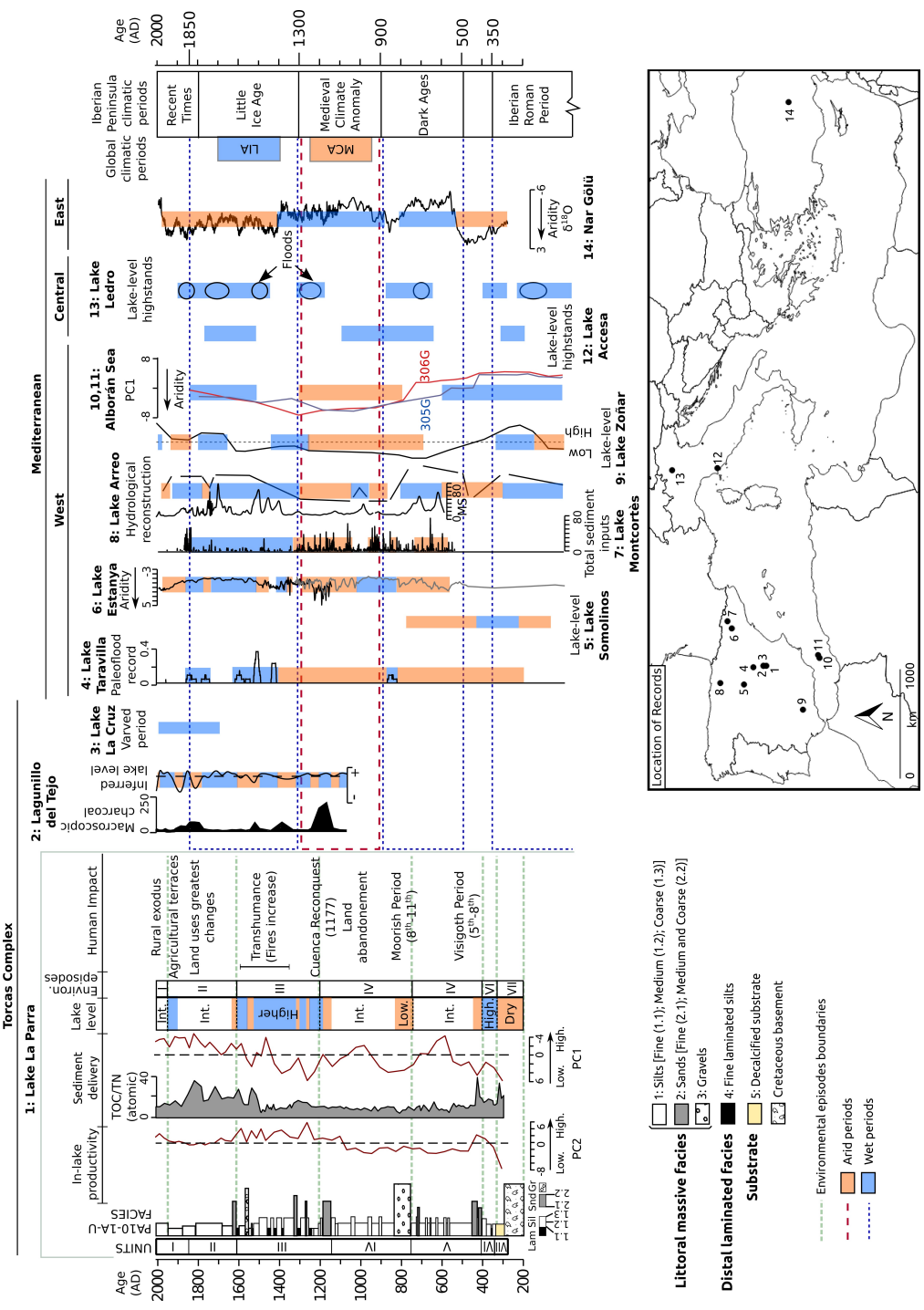

Figure 2. Lake La Parra sedimentary PA10-1A-U sequence in calibrated years AD/BC (dates are based on AMS ^{14}C and ^{210}Pb dating), with subdivision in units and sedimentological profile. The global North hemisphere Medieval Climate Anomaly (MCA) and Little Ice Age (LIA) are represented following the chronology of Mann et al. (2009). Chronology for main Iberian Peninsula climatic periods is based on Martín-Puertas et al. (2008), Moreno et al. (2012) and Morellón et al. (2011). Changes in sedimentary delivery to the lake are represented by TOC/TN (atomic) profile (in dark gray) and the negative values of PC1 (red line). Lake level fluctuations (dry, intermediate and high) and main paleoenvironmental and paleohydrological episodes explained on text are indicated. Principal human impact and historical events in the study area are shown. The record is compared with available records from the nearby Lagunillo del Tejo (López-Blanco et al., 2011) and Lake La Cruz (Julià et al., 1998) in the Torcas karstic lake Complex; West Mediterranean: Taravilla (Moreno et al., 2008), Somolinos (Currás et al., 2012), Zoñar (Martín-Puertas et al., 2008), Montcortés (Corella et al., 2012), Arreo (Corella et al., 2011, 2013), Estanya (Morellón et al., 2009, 2011) lakes and Alborán Sea records (Nieto-Moreno et al., 2011); and Central Mediterranean: Lake Ledro highstands (Magny et al., 2013) and floods frecuency (Wirht et al., 2013) and Lake Accesa high-stands (Magny et al., 2013) sequences; and East Mediterranean records (Nar Gölü, Jones et al., 2006). Locations on bottom-right map are: 1-La Parra, 2-Lagunillo del Tejo, 3-La Cruz, 4-Taravilla, 5-Somolinos, 6-Estanya, 7-Montcortès, 8-Arreo, 9-Zoñar, 10-Alborán core 305G, 11-Alborán core 306G, 12-Accesa, 13-Ledro, 14-Nar Gölü.